RECENT RESULTS FROM DASP ON e^+e^- ANNIHILATION (II)

Günter Wolf*
Deutsches Elektronen-Synchrotron DESY,
Hamburg

Abstract:

Inclusive production of $\pi^{\pm}$, $K^{\pm}$ and $\bar{p}$ by e^+e^- annihilation has been analyzed for cm energies W between 3.6 and 5.2 GeV. The experimental information on the F and F* mesons is reviewed including new data on $F\bar{F}$ production at 4.16 GeV. Data are presented on semileptonic decays of charmed particles. Electron-two-prong data have revealed τ production at the ψ' which is below charm threshold. With these data a precise value for the τ mass has been obtained, $m_{\tau} = 1.807 \pm 0.020$ GeV. Leptonic and semileptonic decay modes of the τ are discussed.

The members of the DASP collaboration are
R. Brandelik, W. Braunschweig, H.-U. Martyn, H.G. Sander, D. Schmitz, W.Sturm, and W. Wallraff, I. Physikalisches Institut der RWTH Aachen,
D. Cords, R. Felst, R. Fries, E. Gadermann, H. Hultschig, P. Joos, W. Koch, U. Kötz, H. Krehbiel, D. Kreinick, H.L. Lynch, W.A. McNeely, G. Mikenberg, K.C. Moffeit, D. Notz, R. Rüsch, A. Shapira, M. Schliwa, B.H. Wiik, and G. Wolf, Deutsches Elektronen-Synchrotron DESY, Hamburg,
J. Ludwig, K.H. Mess, A. Petersen, G. Poelz, J. Ringel, O. Römer, K. Sauerberg, and P. Schmüser, II. Institut für Experimentalphysik der Universität Hamburg,
W. De Boer, G. Buschhorn, W. Fues, Ch. v. Gagern, G. Grindhammer, B. Gunderson, R. Kotthaus, H. Lierl, and H. Oberlack, Max-Planck-Institut für Physik und Astrophysik, München,
S. Orito, T. Suda, Y. Totsuka, and S. Yamada, Lab. of Int. Coll. on Elementary Particle Physics and Department of Physics, University of Tokyo.

1. INTRODUCTION

New results from DASP on the total hadronic cross section, on the p_c/χ states and on the radiative J/ψ decays are discussed by G. Grindhammer[1] at this meeting. This lecture concentrates on inclusive particle production, the evidence for F and F^*, the semileptonic decays of charmed particles, and the properties of the τ. Most of the information presented here was obtained after the 1977 Hamburg conference[2].

2. INCLUSIVE HADRON PRODUCTION AND A TEST FOR SCALING

One of the basic properties of electron hadron scattering is the almost perfect scale invariance exhibited by the structure functions in the deep inelastic region. Inclusive hadron production in e^+e^- annihilation is expected to possess similar properties. First measurements on this subject were carried out by the SLAC-LBL collaboration who observed approximate scaling of the sum over all charged hardons produced[3]. In the DASP experiment[4] the $\pi^\pm$, $K^\pm$ and $\bar{p}$ spectra were determined separately, which allowed to test scaling for each particle species.

2.1 Kinematics

We start with a brief description of the formalism[5] for inclusive hadron production

$$e^+e^- \to h^\pm X \qquad (2.1)$$

depicted in the following figure:

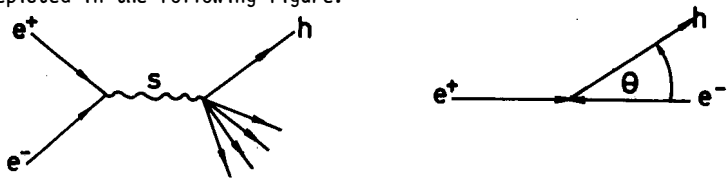

Define:

q	=	$p_+ + p_-$	four momentum vector of the virtual photon
q^2	=	s	square of the cm energy
p	=	$(\vec{p},E)$	four momentum vector of the hadron h
Θ	=	production angle of h with respect to the e^+ direction	
x	=	$\frac{2q \cdot p}{s} = \frac{2E}{\sqrt{s}}$	fractional energy of h
ν	=	$\frac{q \cdot p}{m} = \frac{E}{m}\sqrt{s}$	energy of γ in h rest system

Note that $\frac{2m\nu}{s} = x$.

The virtual photon, as seen in the rest system of h, has transverse (T) and longitudinal (L) components. As a consequence the process (2.1) is described by two independent structure functions, e.g. $\bar{W}_T$ (s,ν) and $\bar{W}_L$ (s,ν). The differential cross section has the form

$$\frac{d^2\sigma}{dx\, d\Omega} = \frac{\alpha^2}{s} \frac{|\vec{p}|}{\sqrt{s}} m \{\bar{W}_T (1 + \cos^2\Theta) + \bar{W}_L (1 - \cos^2\Theta)\} \tag{2.2}$$

Special cases of (2.2) are pair production of fermions (e.g. $e^+e^- \to \mu^+\mu^-$) where $\bar{W}_L = 0$ and of scalar or pseudoscalar mesons (e.g. $e^+e^- \to \pi^+\pi^-$), where $\bar{W}_T = 0$. It is customary to use instead of $\bar{W}_L$, $\bar{W}_T$ the structure fucntions $\bar{W}_1$ and $\bar{W}_2$ which are defined as:

$$\bar{W}_1 (s,\nu) = \bar{W}_T (s,\nu) \tag{2.3}$$

$$\bar{W}_2 (s,\nu) = \frac{m^2}{|\vec{p}|^2} (\bar{W}_L (s,\nu) - \bar{W}_T (s,\nu) \tag{2.4}$$

Note that in the pure transverse case ($\bar{W}_L = 0$) the equivalent of the Callan-Gross relation reads

$$\nu\bar{W}_2 = - \frac{2m}{x\beta^2} \bar{W}_1 \tag{2.5}$$

From (2.2) and (2.4) we find

$$\frac{d^2\sigma}{dx\, d\Omega} = \frac{\alpha^2}{s} \beta x \{m \bar{W}_1 + \frac{1}{4} \beta^2 x \nu\bar{W}_2 \sin^2\Theta)\} \tag{2.6}$$

where $\beta = |\vec{p}| / E$. Note that $m\bar{W}_1 \geq 0$ since the cross section has to be a positive quantity. After integrating over the angles and replacing $4\pi\alpha^2/3s$ by $\sigma_{\mu\mu}$ one has

$$\frac{d\sigma}{dx} = 3\sigma_{\mu\mu} \beta x \{m \bar{W}_1 + \frac{1}{6} \beta^2 x \nu\bar{W}_2\} \tag{2.7}$$

For E >> m this simplifies to

$$\frac{d\sigma}{dx} = 3\sigma_{\mu\mu} x \{m \bar{W}_1 + \frac{1}{6} x \nu\bar{W}_2\} \tag{2.8}$$

If the structure functions $\bar{W}_1$ and $\bar{W}_2$ obey scaling they become functions of the ratio ν/s alone. Using $x = \frac{2m\nu}{s}$ as the scaling variable and substituting

$$\begin{aligned} - m\bar{W}_1 (s,\nu) &\equiv \bar{F}_1 (x,s) \\ \nu\bar{W}_2 (s,\nu) &\equiv \bar{F}_2 (x,s) \end{aligned} \tag{2.9}$$

scale invariance is defined as

$$\lim_{\substack{\nu \to \infty \\ x = \text{const}}} m\bar{W}_1(s,\nu) = \lim_{\substack{s \to \infty \\ x = \text{const}}} \bar{F}_1(x,s) \equiv \bar{F}_1(x) \tag{2.10}$$

and similarly

$$\lim \nu\bar{W}_2(s,\nu) = \bar{F}_2(x).$$

Scale invariance leads to the following expression for the inclusive cross section:

$$\frac{d\sigma}{dx} = 3\sigma_{\mu\mu} x \{-\bar{F}_1(x) + \frac{1}{6} x \bar{F}_2(x)\} \tag{2.11}$$

If scale invariance is valid the shape of the particle energy spectra, $d\sigma/dx$, is independent of s. Furthermore, the magnitude of the inclusive cross section behaves like s^{-1}.

2.2 Experimental Procedure

The inclusive spectra measured by DASP[4] were obtained employing a genuine inclusive trigger: besides a charged particle in one of the spectrometer arms no other requirement was imposed on the final state. A detailed description of the particle identification can be found in Ref. 4. Basically, particles penetrating the iron filter were identified as muons; electrons were recognized by shower, cerenkov and time-of-flight counters; pions, kaons and protons (antiprotons) were identified by time-of-flight. The momentum range was for pions 0.14-1.5 GeV/c, for kaons 0.28-1.6 GeV and for protons (antiprotons) 0.45-3 GeV/c.

Data were taken at cm energies between 3.6 and 5.2 GeV for a total luminosity of ~ 8100 nb^{-1}. They were grouped into eight different energy intervals. A total of ~10^4 $\pi^{\pm}$, ~10^3 $K^{\pm}$ and 130 $\bar{p}$ were used for the analysis. Since the majority of the protons were due to beam gas interactions only antiprotons were considered. The proton yield was assumed to be the same as for antiprotons.

The differential cross section for inclusive production in general depends on the polar angle Θ (see e.g. eq. (2.6)). In the present analysis the polar angular acceptance was $|\cos\Theta| < 0.55$. Within this range no statistically significant $\cos\Theta$ dependence was observed and a constant angular

distribution was assumed in order to integrate the cross section over $\cos\Theta$.

To estimate the possible error introduced by this procedure we consider the limit that only transverse photons contribute, $W_L = 0$. In this case the cross sections given below would have to be increased by at most 24 %. With the angular dependence observed by SLAC-LBL[3] the estimated increase is less than 5 % for $x \lesssim 0.5$ and ≈13 % above.

2.3 General Behaviour of Inclusive Particle Production

Fig. 2.1 gives an impression of the relative frequency of pions, kaons and nucleons. It shows the cross sections $d\sigma/dp$ as a function of momentum for the individual types of particles averaged over cm energies between 4 and 5.2 GeV. (Here $d\sigma/dp$, e.g. for $\pi^\pm$ means the sum for π^+ and π^- production.) The dashed curves were obtained from an extrapolation of the invariant cross sections $E/4\pi p^2\, d\sigma/dp$ (see below). They indicate the expected momentum dependence at low momenta, where the particles are swept out of the spectrometer due to the magnetic field (pions), are lost by decay (kaons) or suffer too big an energy loss in the material in front of the magnet (antiprotons). Below 0.5 GeV/c the $\pi^\pm : K^\pm : 2\bar{p}$ yields are roughly in the ratio 100 : 10 : 1. With increasing momenta the differences become smaller.

Fig. 2.2 shows the same data plotted in terms of the invariant cross section $E\, d^3\sigma/d^3p \equiv E/4\pi\, p^2\, d\sigma/dp$. To within 20 or 30 % accuracy the $\pi^\pm$, $K^\pm$ and $2\bar{p}$ fall on the same curve which is well approximated by an exponential,

$$E/4\pi p^2 \quad d\sigma/dp \quad \sim \exp(-bE)$$

The exponent b has the value 5.4 GeV^{-1}. A similar behaviour was observed for the inclusive spectra from J/ψ decay (see Fig. 2.3)[6]. Inclusive spectra in hadronic collisions behave in the same way if the data are plotted as a function of the transvers energy $E_T = \sqrt{m^2 + p_\perp^2}$. This is demonstrated in Fig. 2.3 where the curves represent the inclusive spectra from pp collisions in the central region at $\sqrt{s} = 53$ GeV. It is surprising to see that inclusive spectra that come from such different initial states as e^+e^- collisions, J/ψ decay and pp collisions are very similar.

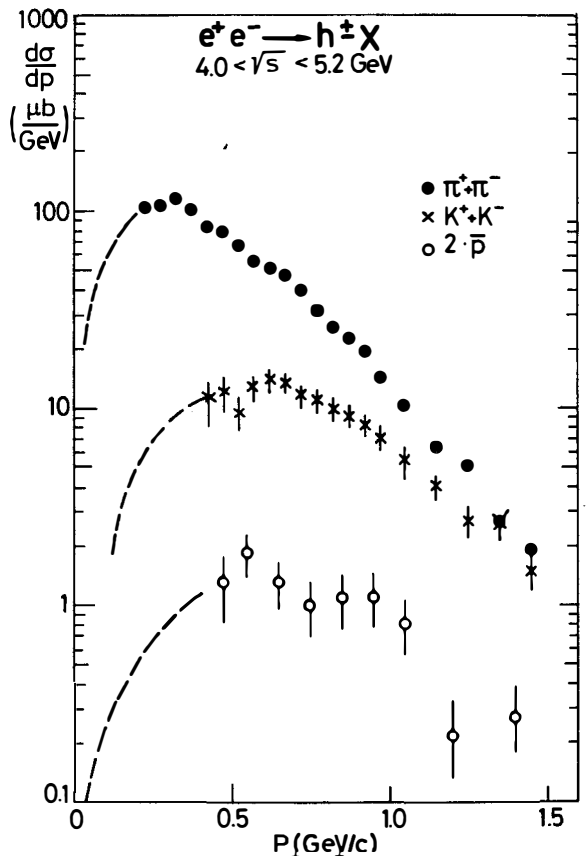

2.1 Momentum spectra of $\pi^\pm$, $K^\pm$ and $\bar{p}$ as measured by DASP

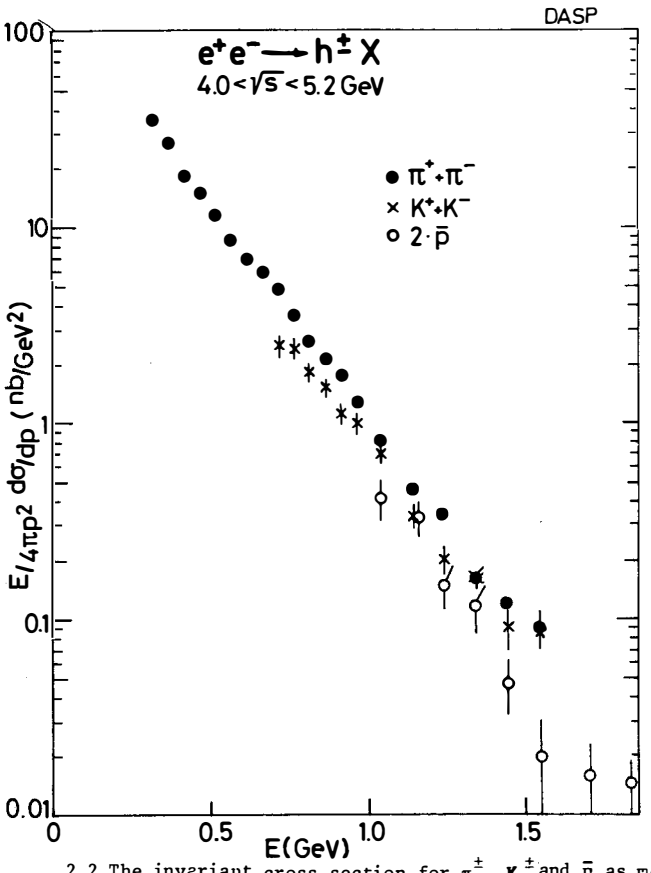

2.2 The invariant cross section for $\pi^\pm$, $K^\pm$ and $\bar{p}$ as measured by DASP

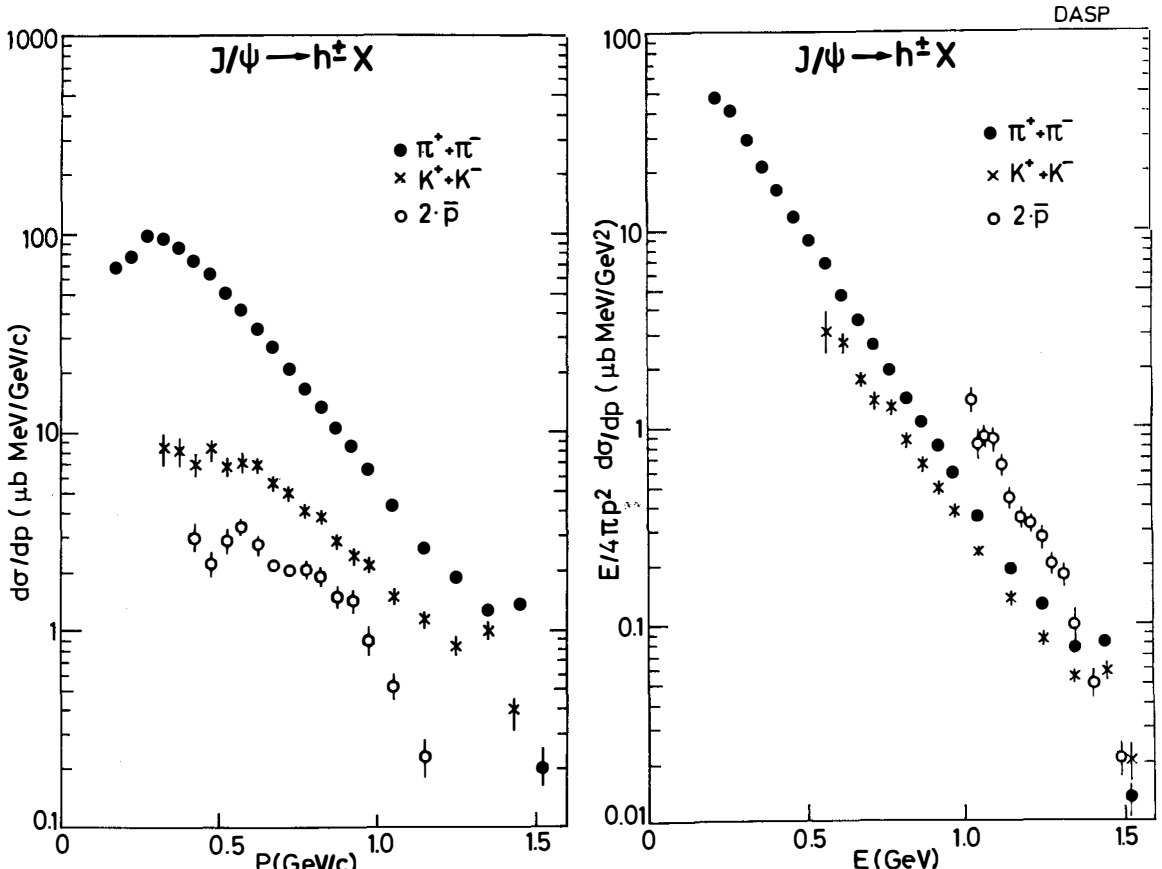

2.3 The momentum spectra and invariant cross sections for the sum of $\pi^{\pm} + \pi^{\pm}$, $K^{+} + K^{-}$ and $2.\bar{p}$ from J/ψ decay (Ref. 6).

2.4 Test for Scaling

Since the angular distribution was found to be consistent with isotropy we neglect the second term in eq. (2.6) and obtain

$$\frac{d\sigma}{dx} \simeq \frac{4\pi\alpha^2}{s} \beta x \bar{W}_1 (s,\nu) \qquad (2.12)$$

The quantity $\frac{s}{\beta}\frac{d\sigma}{dx}$ is then proportional to the structure function $\bar{W}_1$. For the purpose of orientation Fig. 2.4 shows first the ratio $R = \sigma_{tot}/\sigma_{\mu\mu}$ in the energy region analyzed here[1]. Note that the heavy lepton contribution has been excluded. At 3.6 GeV which is the first energy analyzed and which is below charm threshold, R is of the order of 2.3. Above charm threshold three resonance-like structures show up at 4.04, 4.16 and 4.41 GeV. Beyond 4.5 GeV R seems to have reached its post charm level with a value of 4.5.

Fig. 2.5 shows the x dependence of $\frac{s}{\beta}\frac{d\sigma}{dx}$ for $\pi^{\pm}$(i.e. sum of π^+ and π^-), $K^{\pm}$ and twice the $\bar{p}$ production as measured in the eight energy intervals. The π, K and $\bar{p}$ cross sections for $x \gtrsim 0.2$ decrease nearly exponentially. Moreover, with increasing energy $\sqrt{s}$, and increasing x the cross sections for the three particle species become more and more alike. The $\bar{p}$ data, within large errors, do not show any significant change with s, i.e. they appear to scale.

In order to test the pion data for scaling we compare in Fig. 2.6 the cross sections at the "nonresonant" energies s = 13 and 25 GeV^2. Below $x \simeq 0.3$ the cross section rises by a factor of 1.5 to 2 between s = 13 and 25 GeV^2. At higher x values the two cross section sets agree within errors. In other words, the rise of R from a value of 2.3 at s = 13 GeV^2 to ~ 4.5 at 5.0 GeV is associated with low x pions only.

In Fig. 2.7 $(s/\beta)\, d\sigma/dx$ is plotted for $\pi^{\pm}$ and $K^{\pm}$ as a function of s for fixed x. A large increase in the π cross section at s = 16 GeV^2 is most prominent for $x < 0.4$. The cross sections at s = 13 and 27 GeV^2 for $x \gtrsim 0.4$ are equal within errors. The K cross sections increase by a factor of two or three from s = 13 to s = 16 GeV^2. For $x > 0.4$ the K cross section above the 4 GeV resonance region falls back to its pre-charm level. This suggests that at high energies ($s > 30$ GeV^2) charm contributions to K production are confined to x values below 0.4. Note also that for $s \gtrsim 25$ GeV^2 and $x \geq 0.3$ π and K cross sections tend to be the same.

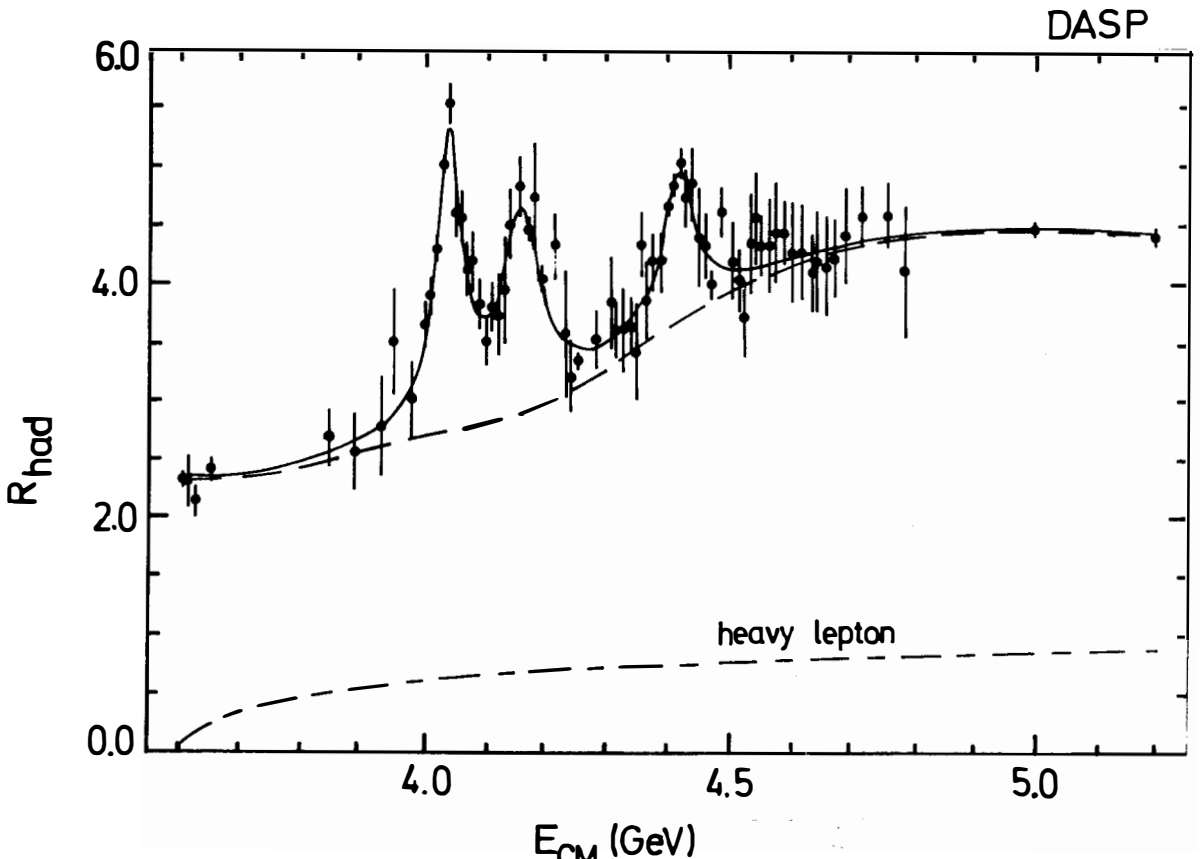

2.4 $R = \sigma^{tot}/\sigma_{\mu\mu}$ without the heavy lepton contribution as measured by DASP (Ref. 4)

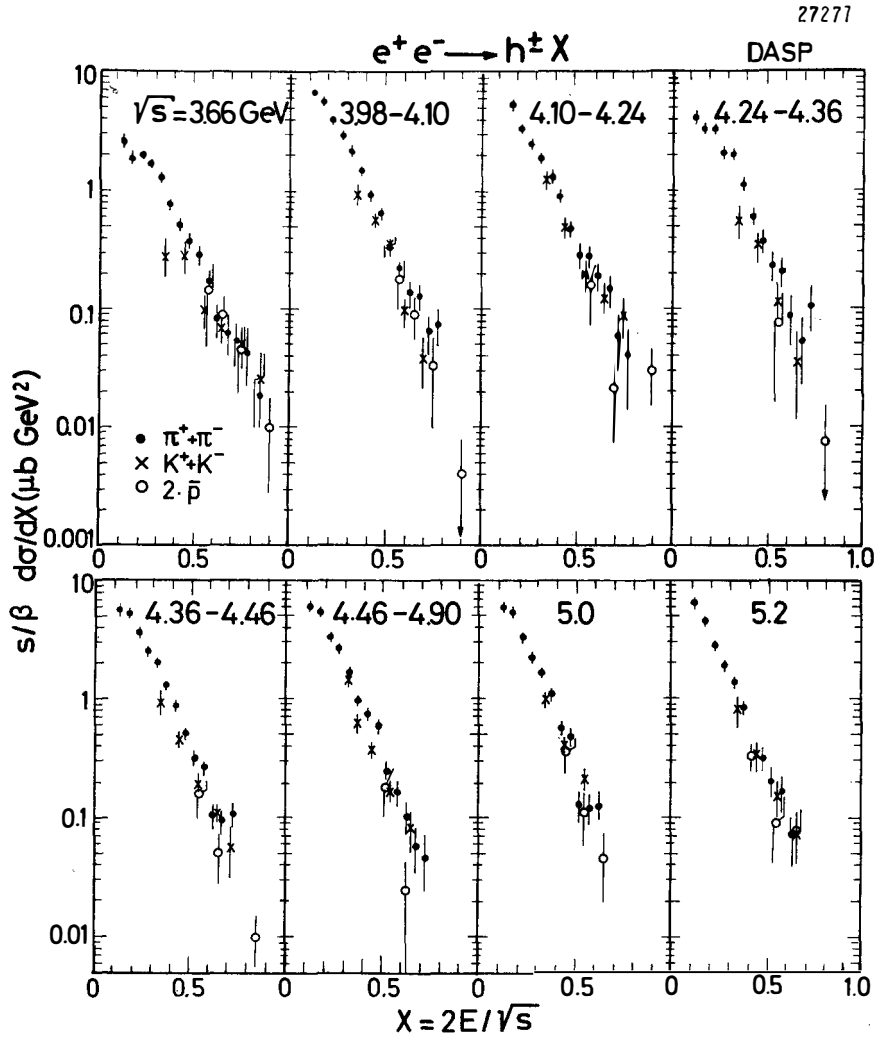

2.5 The cross section $(s/\beta)d\sigma/dx$, $x \equiv 2E/\sqrt{s}$, versus x for the sum of π^+ and π^-, K^+ and K^-, and twice the $\bar{p}$ yield, as measured by DASP (Ref.4).

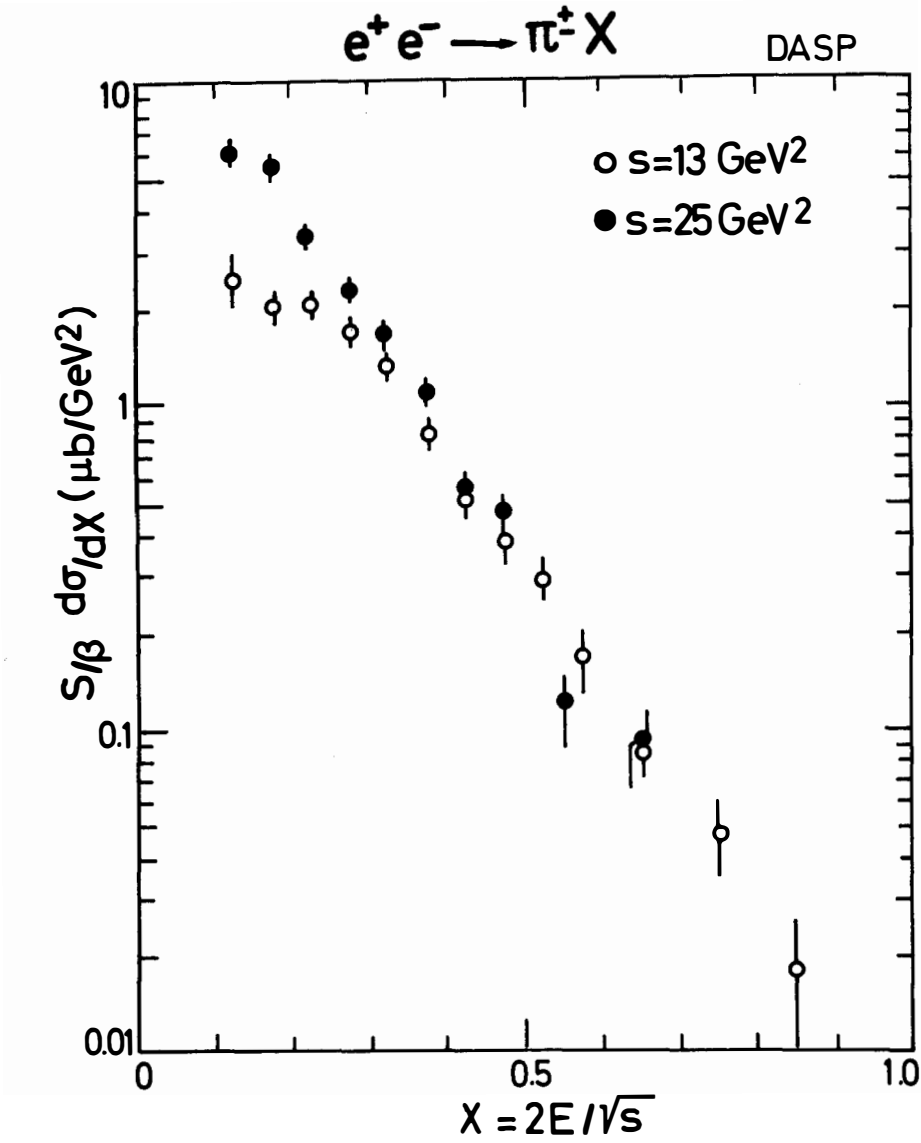

2.6 Comparison of the crsoss section $s/\beta \; d\sigma/dx$ for $\pi^\pm$ production at $s = 13$ and 25 GeV^2 (Ref. 4).

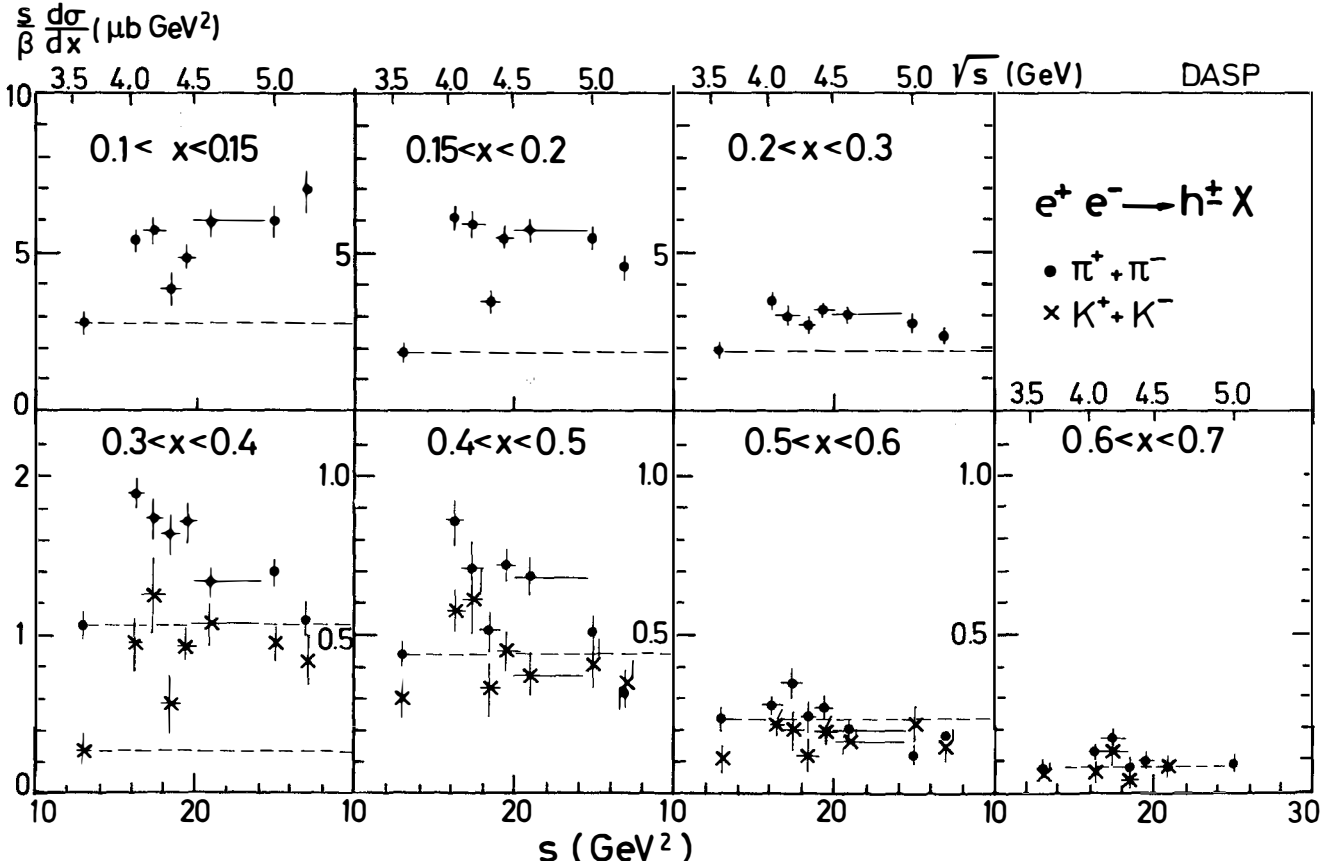

2.7 The cross section $(s/\beta)\, d\sigma/dx$ versus s for fixed x for $\pi^\pm$ and $K^\pm$ production as measured by DASP (Ref. 4).

2.5 $e^+e^- \to \bar{p}X$ and $e\,p \to e'X$

Inclusive production of a particle h by e^+e^- annihilation and inelastic electron scattering on particle h are related by crossing (see diagrams below). At the special point x = 1 (where for inelastic electron scattering x is defined as $2\,p \cdot q\,/(-q^2)$, q, p four momenta of the virtual photon and the target particle h) the structure functions for one process can be calculated from those of the other one if scaling holds. Consider $e^+e^- \to \bar{p}X$ and $e\,p \to e'X$. In this case[5]

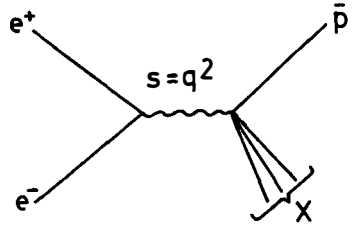

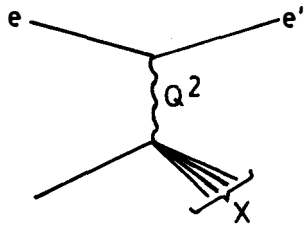

$e^+e^- \to pX$

$$\bar{F}_1\,(x = 1) = -\,F_1(x = 1)$$
$$\bar{F}_2\,(x = 1) = \;\;F_2(x = 1) \qquad (2.13)$$

$e\,p \to e'X$

However, an analytic continuation which would connect points at $x \neq 1$ is in general not possible[7].

Gribov and Lipatov[8], studying both processes in a field theoretical model predicted the following relations:

$$\bar{F}_1(x) = \frac{-1}{x}\;F_1\left(\frac{1}{x}\right)$$
$$\bar{F}_2(x) = \frac{1}{x^3}\;F_2\left(\frac{1}{x}\right) \qquad (2.14)$$

A preliminary analysis of the DASP data for $F_2(x)$ is shown in Fig. 29. The experimental points were obtained by summing over cm energies from 4 to 5.2 GeV. The structure function $\bar{F}_2(x)$ was determined from the data assuming the Callan-Gross relation

$$x\bar{F}_2(x) = -\bar{F}_1(x) \qquad (2.15)$$

which leads to

$$\frac{d\sigma}{dx} = \frac{3}{2}\;\sigma_{\mu\mu}\beta(1 - \beta^2/3)\;x\;\;\bar{F}_2(x) \qquad (2.16)$$

The Gribov-Lipatov prediction calculated from deep inelastic ep scattering data is shown by the curve in Fig. 2.8. It fails to describe the data: the

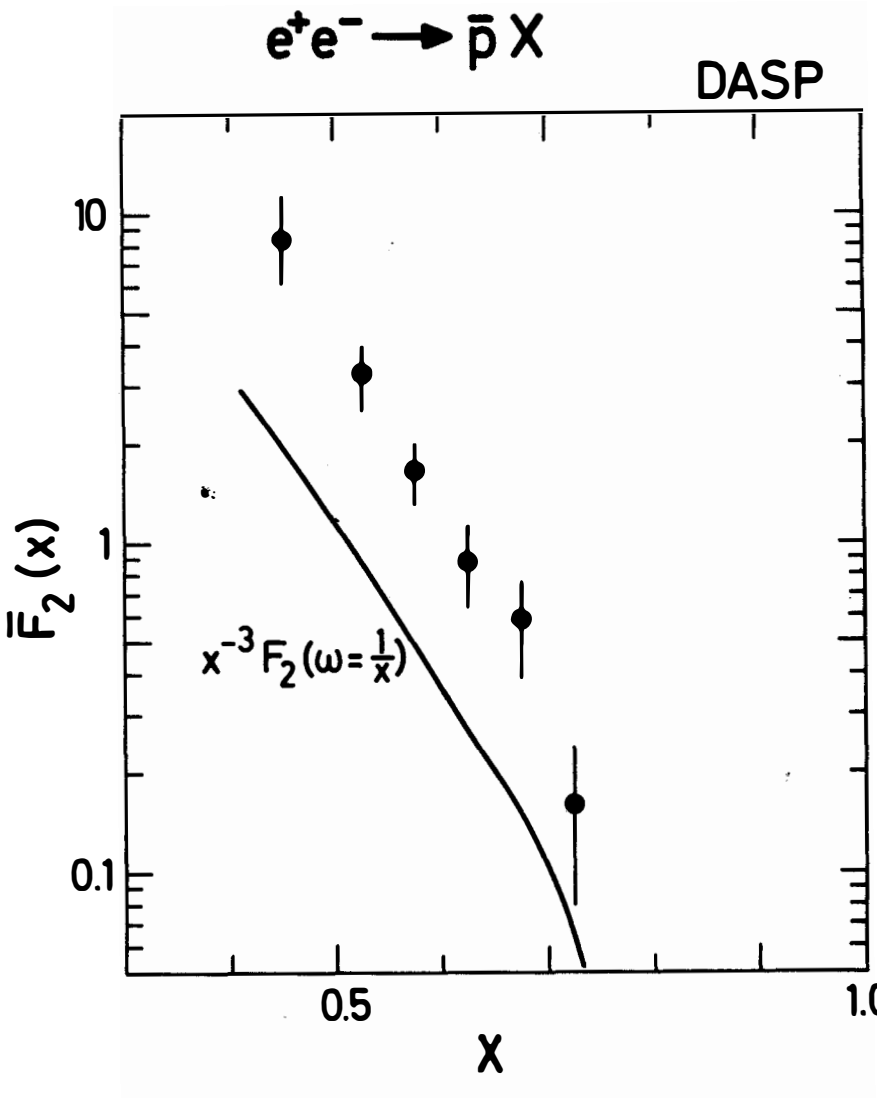

2.8 The structure function $\bar{F_2}(x)$ for $e^+e^- \to \bar{p}X$ as obtained from a preliminary analysis of DASP. The curve shows the prediction of Gribov-Lipatov.

theoretical curve is always below the measured points. The discrepancy is a factor of ~2 at x = 0.8 rising to ~4 at x = 0.4. Part of this failure - if not all - may have to be attributed to contributions from processes of the type

$e^+e^- \rightarrow h\,X,\ h\ \bar{p} + \ldots$ where $h = \Lambda_{\bar{p}\ldots}, \Sigma_{\bar{p}\ldots}, N_{\bar{p}\ldots}$, etc.

which should be excluded from the e^+e^- data before the comparison is being made. It is this type of contributions which prevent in general an analytic continuation from the scattering to the annihilation case[7].

3. THREE GLUON VERSUS $q\bar{q}$ ANNIHILATION

Approximately 70 % of the J/ψ decays are direct decays into hadrons which are believed to proceed via three gluon annihilation. Electron-positron annihilation into hadrons on the other hand at high energies appears to proceed via a primary quark-antiquark pair. For this reason one might expect the J/ψ to yield more low energy particles than nonresonant hadron production. DASP[6] has analyzed the inclusive spectra for $\pi^\pm$, $K^\pm$ and $\bar{p}$ from J/ψ decay and for a cm energy $\sqrt{s}$ of 3.6 GeV (i.e. below charm threshold). In Fig. 3.1 the cross section $\frac{1}{\sigma_{tot}} \frac{1}{\beta} \frac{d\sigma}{dx}$ is shown as a function of the fractional particle energy $x \equiv 2E/\sqrt{s}$. The data points represent the values at 3.6 GeV, the curves the result at the J/ψ. The J/ψ curves were normalized such that the integrated π cross section from J/ψ agrees with that at 3.6 GeV for x = 0.3. Within errors no difference is observed in the shape of the π and K spectra at the two energies. Most likely the energy of ~3 GeV is too low for the two mechanisms to produce a noticecable difference. Remember that at 3 GeV the sphericity distributions for the two extreme cases of phase space and jet formation are the same[9].

The only difference between on and off resonance data in Fig. 3.1 is seen to occur for antiprotons. The J/ψ decay relative to the π and K yields produces more antiprotons by a factor of 2-3. No explanation has been offered for this fact.

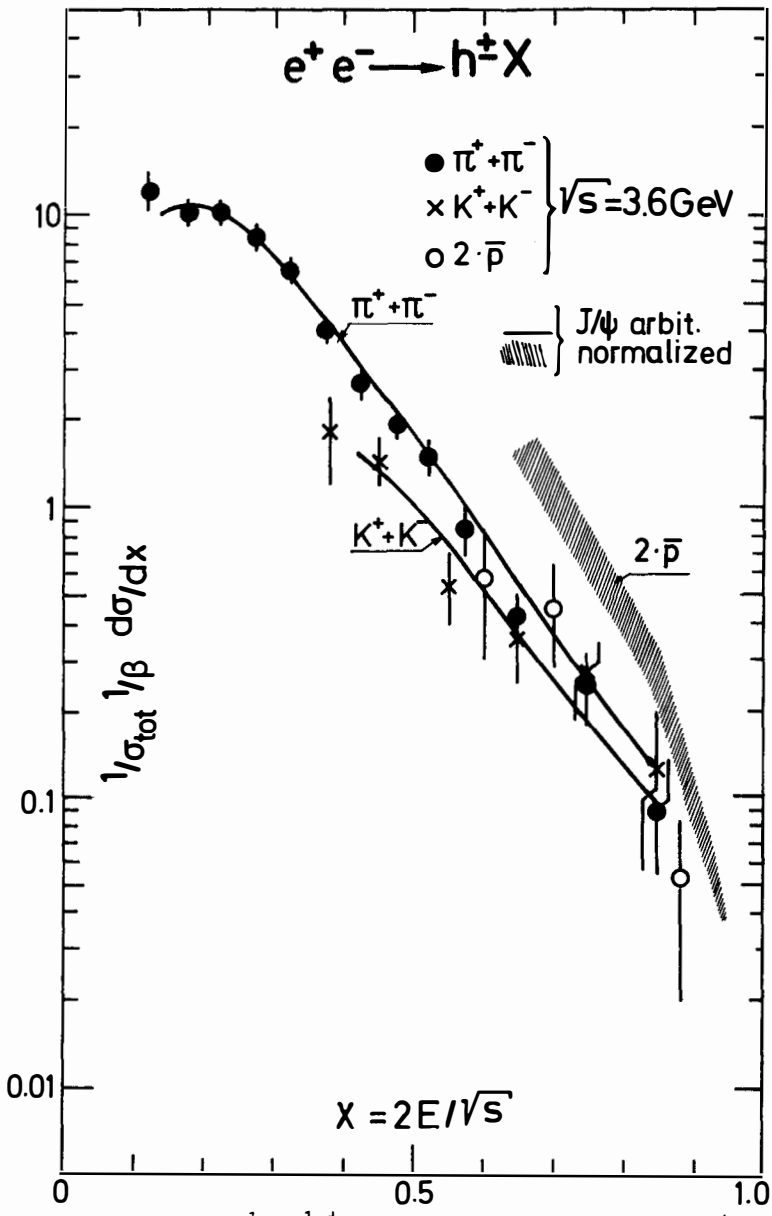

3.1 The cross section $\frac{1}{\sigma_{tot}} \frac{1}{\beta} \frac{d\sigma}{dx}$ versus $X = 2E/\sqrt{s}$ for the sum of $\pi^+ + \pi^-$, $K^+ + K^-$ and twice the $\bar{p}$ yield at 3.6 GeV (data points) and from J/ψ decay (curves) measured by DASP[6]. The J/ψ data have been normalized by a common normalization factor.

4.1 The F mesons

The charm model predicts mesons carrying both charm and strangeness. The ground state is F^+. The GIM favored decay of the F is into an $s\bar{s}$ system leading to final states containing $K\bar{K}, \Phi$, η or η'.

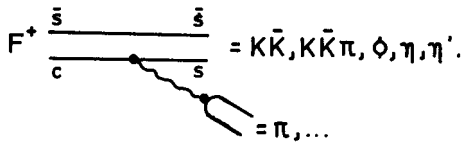

Sizeable η production is therefore a hint for F production. The production characteristics for F mesons can be expected to be similar to that for D's. Copious D production was found near the D^+ threshold at 4.028 GeV proceeding mainly via DD^* and D^*D^* formation. Assuming a similar behaviour for the F meson one expects large FF^* and F^*F^* cross sections near threshold. Since both, F and F^* are isospin singlets the favored decay of the F^+ is the radiative transition $F^* \to F\gamma$ provided the F^* - F mass difference is less than 2 m_π[10]. The signal for F production can therefore be enhanced by requiring a low energy photon in addition to the η signal.

DASP[11] searched for the F meson by studying events of the type

$$e^+e^- \to \eta\gamma_{low} + \geq 2 \text{ charged tracks} + X$$

The η was identified by its decay into two photons. A search of this type is hampered by the $\gamma\gamma$ mass resolution which in the DASP experiment was 80 MeV, and by the large $\gamma_i\gamma_j$ combinatorial background: on the average there are 2-3 π^0's produced near 4 GeV leading to 4-6 photons or 6-15 two-photon mass combinations. The event selection was done as follows: The photons were detected in the inner detector and their angles and energies measured. The detection efficiency was 50 % at 0.05 GeV rising to 80 % at 0.1 GeV and 95 % above 0.3 GeV. Events accepted were required to have at least two charged tracks coming from the interaction region and at least two photons with energies exceeding 0.1 GeV. The vector sum of the momenta of these two photons was required to be between 0.3 and 1.2 GeV. Events containing a photon of less than 0.14 GeV (γ_{low}) in addition to the two used for forming $m_{\gamma\gamma}$ were called low energy photon events.

Fig. 4.1 shows the $m_{\gamma\gamma}$ distribution for events containing a low energy photon for five energy intervals between 4.0 and 5.2 GeV excluding energies around 4.4 GeV; the 4.4 GeV region (4.36 - 4.48 GeV) is presented in Fig. 4.2. There is a clear η signal at 4.4 GeV not observed at the other energies.

The occurence of η production in association with low energy photons at 4.4 GeV is strongly suggestive of FF^* (F^*F^* production). A search was made for the two body decay of the $F^{\pm}$ into $\eta\pi^{\pm}$ detecting the pion in one of the spectrometer arms. A total of 35 events were found with a pion momentum above 0.6 GeV/c, a $\gamma\gamma$ combination in the η region (0.35 - 0.65) and a low energy photon (this time E_γ < 0.2 GeV). These events were fitted to the reactions

$$e^+e^- \to F^{\pm}F^{*\mp} \to (\pi^{\pm}\eta)\ (F^{\mp}\gamma_{low}) \to (\pi^{\pm}\gamma\gamma)\ (F^{\mp}\gamma_{low}) \qquad (4.1)$$

and

$$e^+e^- \to F^{+*}\ F^{-*} \to (\pi^{\pm}\eta\gamma_{low})\ F^{*\mp} \to (\pi^{\pm}\gamma\gamma\gamma_{low})\ F^{*\mp} \qquad (4.2)$$

These are two constraints fits because of the mass constraint on $m_{\gamma\gamma}$ and the requirement that for (4.1) $\pi\eta$ and the missing vector must have the same mass m_F; for (4.2) the $\pi\eta\gamma_{low}$ system and the missing vector must have the same mass m_{F*}.

A total of 25 events gave a fit to (4.1) with a χ^2 < 8. These events are plotted in Fig. 4.3a as a function of Δ, the difference between the measured and the fitted $\pi\eta$ mass. The distribution peaks at Δ = 0. Cutting at $|\Delta|$ = 0.25 GeV 21 events with $|\Delta|$ < 0.25 GeV are retained. These events are shown in scatter plots (Fig. 4.3b,c) of the mass difference between the recoil mass and the $\pi\eta$ mass versus the $\pi\eta$ mass. The data taken at 4.4 GeV have a cluster of 6 events with a well defined $\pi\eta$ mass and a recoil mass some 100 MeV higher. The background is found to be negligible from the event distribution outside the 4.4 region (Fig. 4.3c). In the latter data no event with a $\pi\eta$ mass compatible with the signal at 4.4 GeV was found for an integrated luminosity five times larger than that at 4.4 GeV. Fig. 4.4 shows a scatter plot of the fitted $\pi\eta$ mass versus the mass of the recoil system and Fig. 4.5 gives the projection onto the $\pi\eta$ mass axis. There are six events which give the same ($m_{\pi\eta}$, m_{recoil}) mass values within errors: $m_{\pi\eta}$ = 2.04 GeV, m_{recoil} = 2.17 GeV, m_{F*} = 2.11 GeV. Allowing for possible systematic uncertainties the best estimates are

$$m_F = 2.03 \pm 0.06 \text{ GeV}$$
$$m_{F*} = 2.14 \pm 0.06 \text{ GeV}$$

The mass difference between F^* and F can be directly determined from the energies of the low energy photon:

$$m_{F*} - m_F = 0.12 \pm 0.04 \text{ GeV}.$$

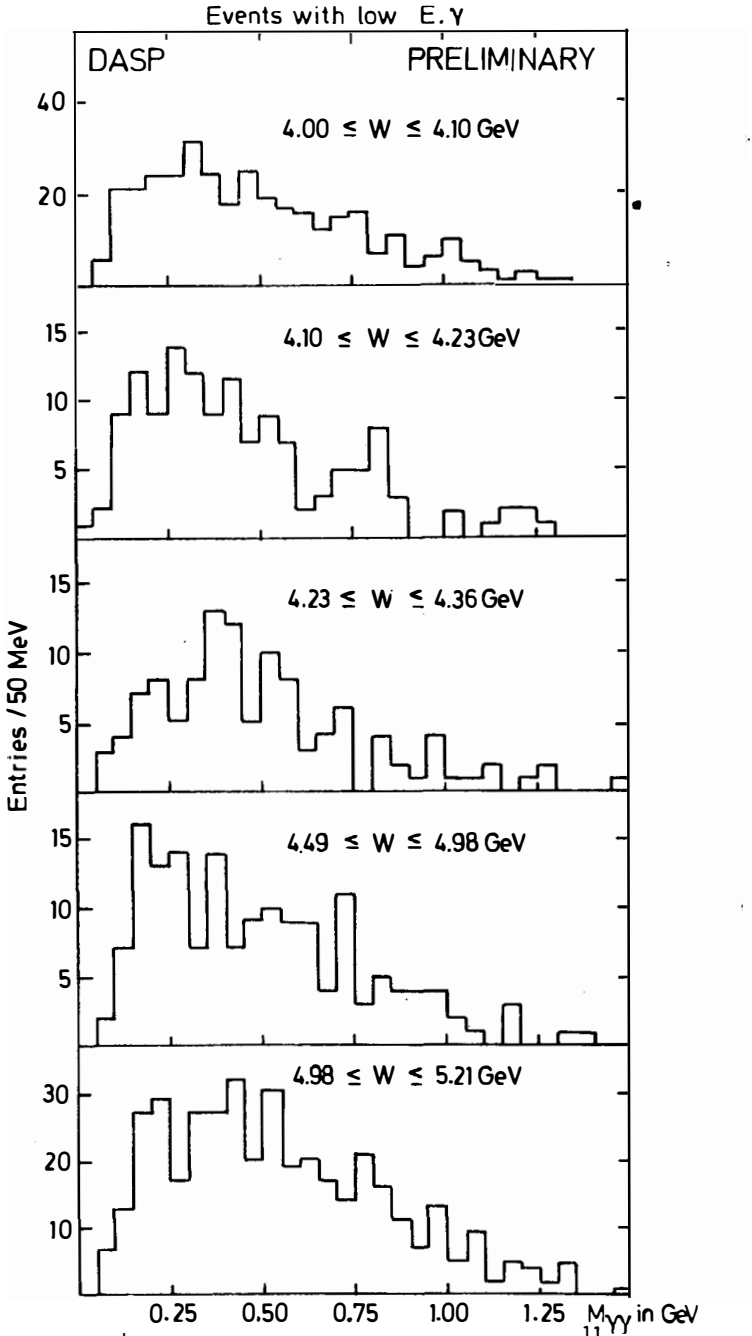

4.1 Reaction $e^+e^- \to \gamma\gamma\gamma + \geq 2$ charged as measured by DASP[11]. The $\gamma\gamma$ low mass distribution for different cm energy intervals.

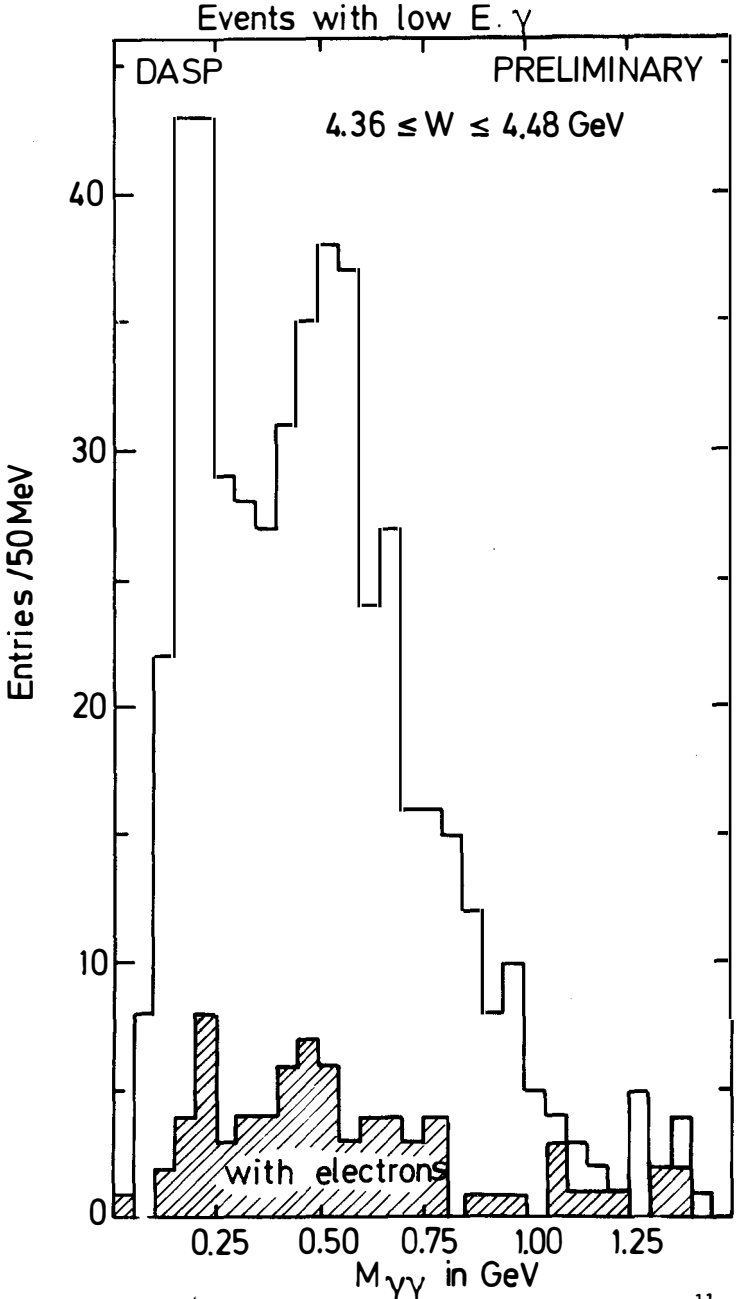

4.2 Réaction $e^+e^- \to \gamma\gamma\gamma_{low} + \geq 2$ charged as measured by DASP[11]. The $\gamma\gamma$ distribution for cm energies between 4.36 and 4.48 GeV.

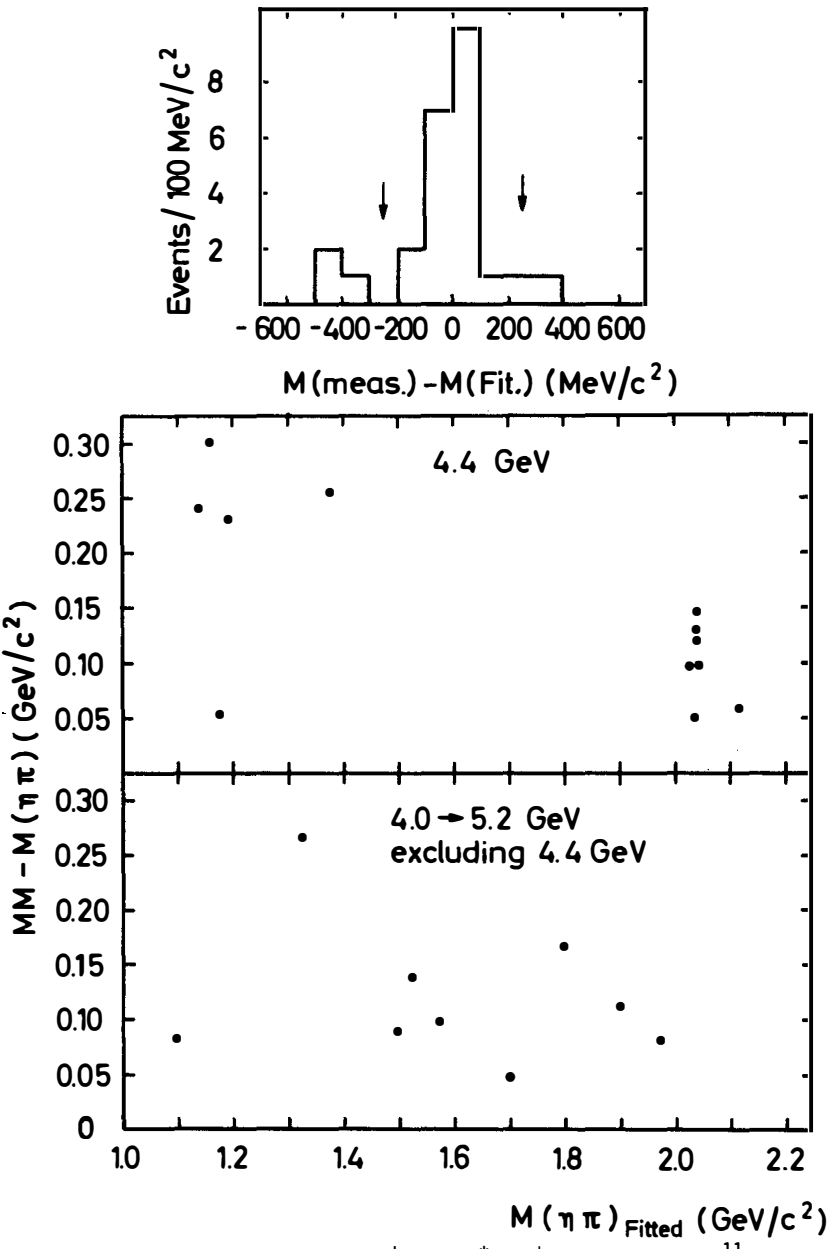

4.3 Results for the fit $e^+e^- \to FF^* \to \pi^\pm \eta \gamma_{low} F$ from DASP[11].
a) difference between measured and fitted $\pi\eta$ mass
b) and c) difference between $\pi\eta$ mass and recoil mass.

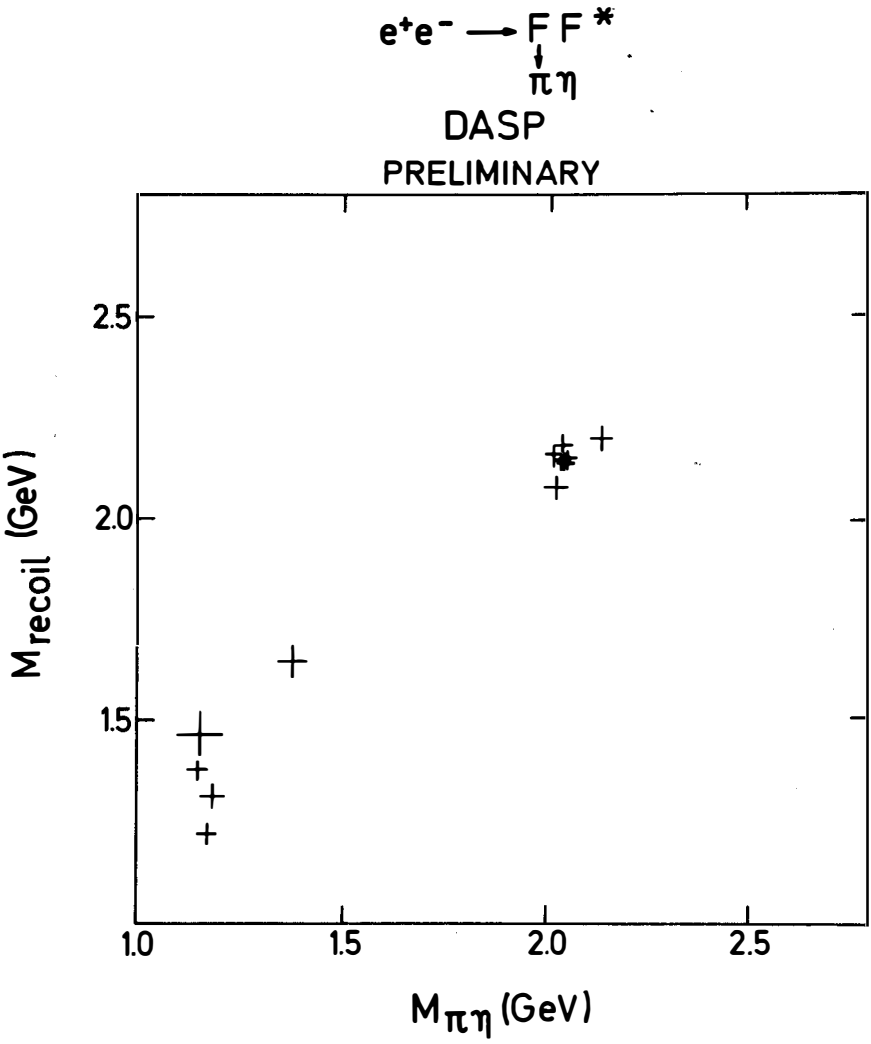

4.4 Results for the fit $e^+e^- \to FF^* \to \pi^\pm \eta \gamma_{low} F$ at 4.4 GeV from DASP[11]. Scatterplot of the fitted F mass versus the F* mass.

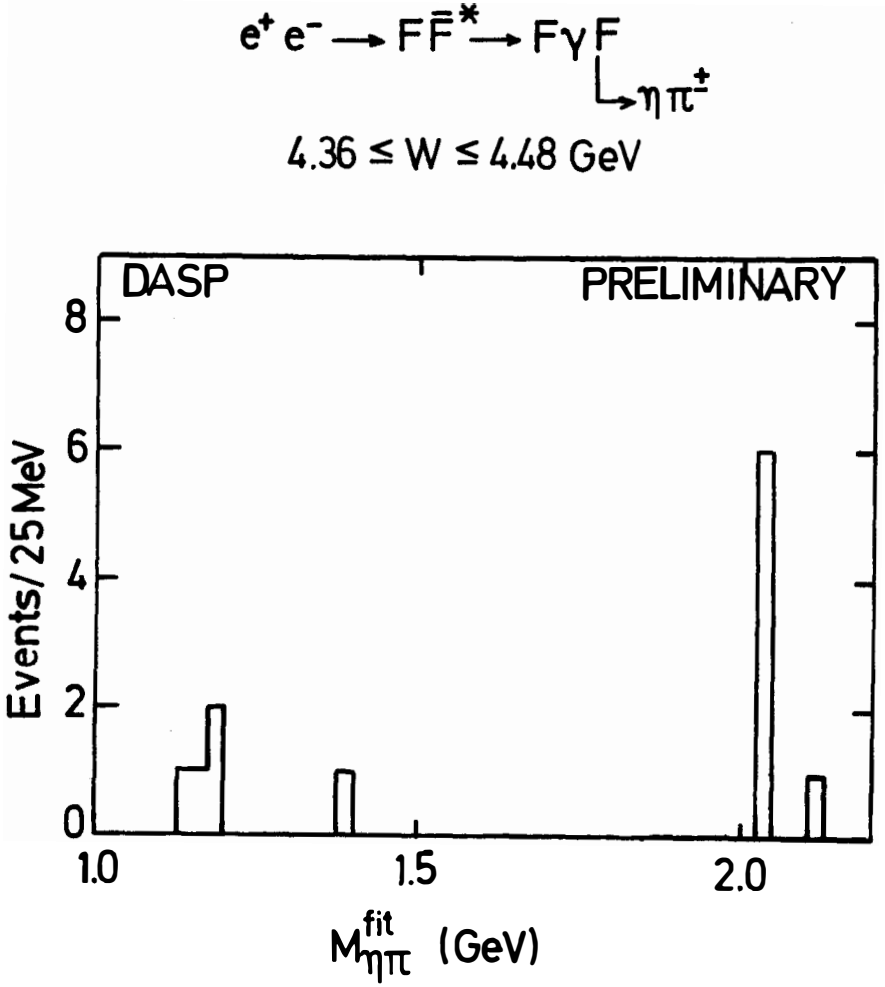

4.5 Results for the fit $e^+e^- \to FF^* \to \pi^\pm\eta\gamma_{low}F$ at 4.4 GeV from DASP[11]. Distribution of the fitted $\pi^\pm\eta$ mass.

By comparison with $D\bar{D}$ production one might expect to find a strong $F\bar{F}$ signal close to the $F\bar{F}$ threshold (~4.06 GeV). In this case no correlation between production of F and a low energy photon will exist. Using the same selection criteria as before but not demanding a low energy photon the $m_{\gamma\gamma}$ mass distribution shown in Fig. 4.6 (cm energy 4.0 - 4.10 GeV) and Fig. 4.7 (4.10 - 4.22 GeV) were obtained. The first energy bin shows a π^0 peak but no η signal. The second energy bin, besides the π^0 exhibits a clear η peak. Since no η signal is observed at 4.0-4.10 GeV the η mesons do not come from D decay and $D\bar{D}\eta$ production is excluded by kinematics.

The observed features strongly suggest to associate the η signal with $F\bar{F}$ production. A search for events with $F^{\pm} \to \pi^{\pm}\eta$ revealed one event. From the fit a value of 2.03 ± 0.01 GeV was found for the F mass.

5. SEMILEPTONIC DECAYS OF CHARMED PARTICLES

5.1 Electron inclusive events

The semileptonic decays of charmed particles were studied with inclusive electron events,

$$e^+e^- \to eX \qquad (5.1)$$

Events of this type can come from charmed particle decays but also from a variety of other sources, trivial ones like QED processes, Dalitz pairs, hadrons faking electrons, or from other new particles such as heavy leptons.
The analysis was done for cm energies between 3.6 and 5.2 GeV and for electron momenta p_e above 0.2 GeV/c.[12,13] The total integrated luminosity amounted to 6300 nb^{-1}. The electron was identified in the magnetic spectrometer by a Cerenkov counter together with either time-of-flight (for $p_e < 0.35$ GeV/c) or shower counters ($p_e > 0.35$ GeV/c). The probability for a pion to fake an electron was measured to be $4 \cdot 10^{-4}$. Electron pairs from Dalitz decay or pair conversion were rejected by pulse height cuts on the scintillation counters mounted before the magnet. Background from QED processes was suppressed by requiring the system X to contain at least one nonshowering track $T^{\pm}$ (e.g. $\mu^{\pm}$, $\pi^{\pm}$, $K^{\pm}$ but not e).
As a result of the selection criteria the trivial background to the events selected turned out to be small (see table 5.1).

In a second step the charged multiplicity distribution and the electron momentum spectra were analysed[12]. It was found that by a simple cut on the multiplicity (shown in Fig. 5.1) a clear separation between events from charmed particle and from heavy lepton decay is possible. Electron events with a single charged track (they will be called electron two prongs) are due basically to heavy leptons; electron events with two or more charged tracks (electron multiprong events) originate from charmed particles. The relevant numbers are

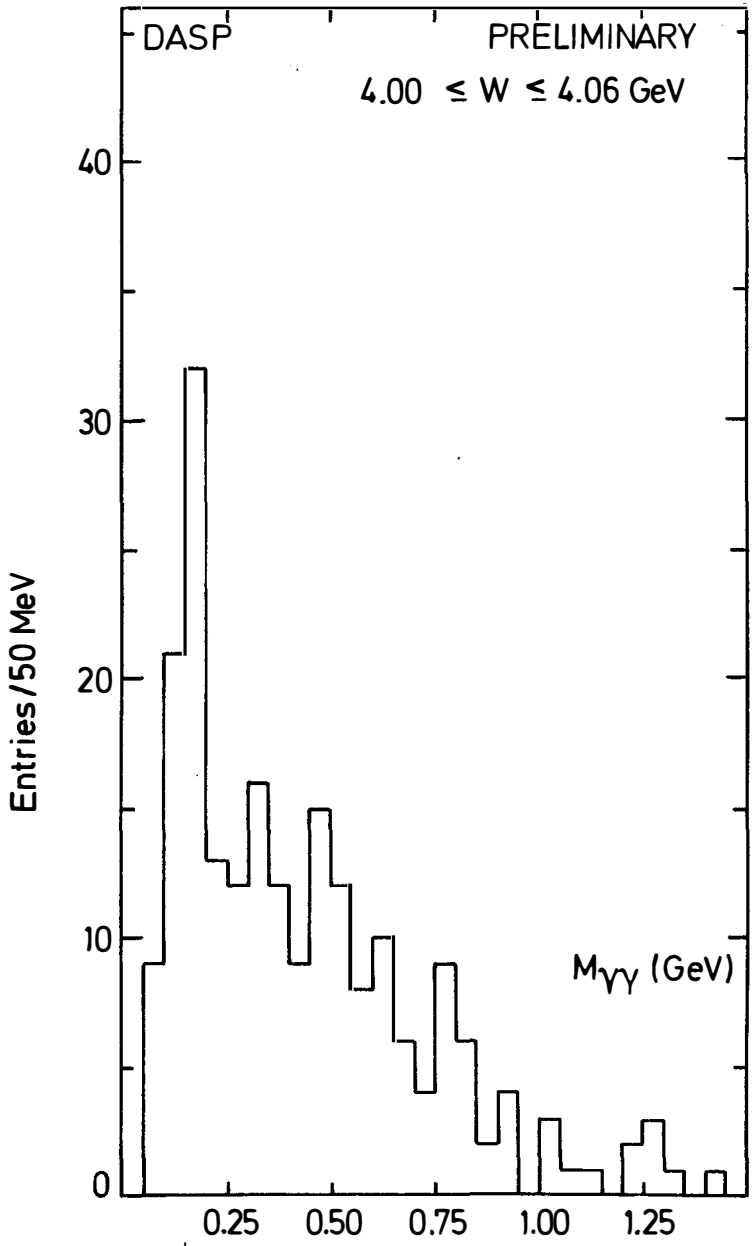

4.6 Reaction $e^+e^- \to \gamma\gamma + \geq 2$ charged for cm energies between 4.0 and 4.1 GeV as measured by DASP[11]

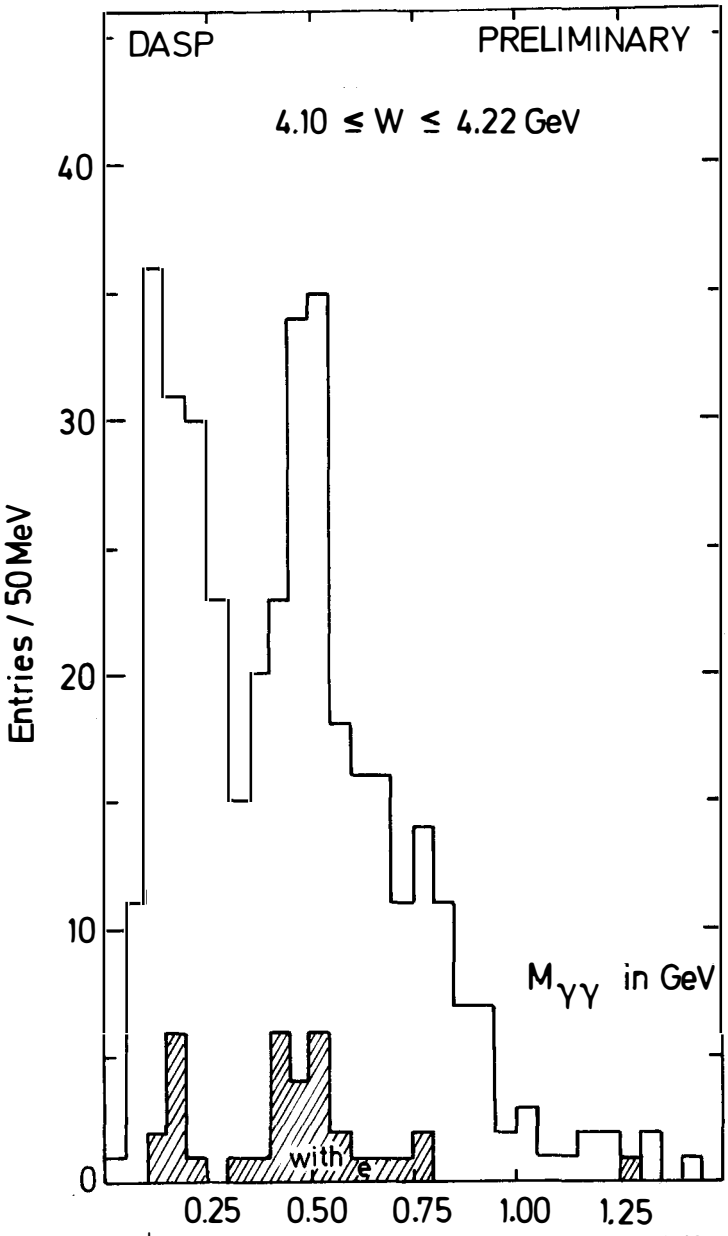

4.7 Reaction $e^+e^- \to \gamma\gamma + \geq 2$ charged for cm energies between 4.10 and 4.22 GeV as measured by DASP[11].

listed in table 5.1. The difference in multiplicity (and electron spectrum as shown below) can be understood (and was expected) in terms of the production and decay characteristics of charmed particles and heavy leptons. This is explained by table 5.2.

Table 5.1 Event statistics for inclusive electron events[12-14]

	Number of events	
	$e^+e^- \to eT^{\pm} n\gamma$, $n \geq 0$	$e^+e^- \to eT^{\pm}$ + charged + $n\gamma$, $n \geq 0$
satisfying selection criteria	60	182
trivial background	7 ± 2	28 ± 9
background from charmed particles	5 ± 2	
background from τ production		<22

Table 5.2 Properties of heavy sequential leptons and new hadrons (taken from Ref. 15)

	L	H
Production	$e^+e^- \to L^+L^-$ (point cross section)	$e^+e^- \to H\bar{H}$ (damped by form factors)
	$e^+e^- \to L^+L^-$ + hadrons (negligible small, less than α^2 of elastic production near threshold)	$e^+e^- \to H\bar{H}$ + hadrons or $H^*\bar{H}^*$ (dominant at higher energies, cross section will have structure)
Decay Modes	$L \to \ell \bar{\nu}_\ell \nu_L$	$H \to \ell \bar{\nu}_\ell$
	$\to \nu_L$ · hadrons	(suppressed if the lowest flavour state has spin 0)
		$\to \ell \bar{\nu}_\ell$ · hadrons
		$\to$ hadrons
Final States:		
$e\mu$ + neutrinos	important, clear signature ($e(\mu)$ from three body decay	negligible ($e(\mu)$ from a multibody decay)
$\ell\ell$ + neutrinos + hadrons	negligible, order α^2 at threshold	large ($e(\mu)$ from a multibody decay)
$e(\mu)$ + neutrino + hadrons	large, lepton spectrum computable and hard, hadrons have low multiplicity	large, lepton spectrum soft, hadrons have high multiplicity

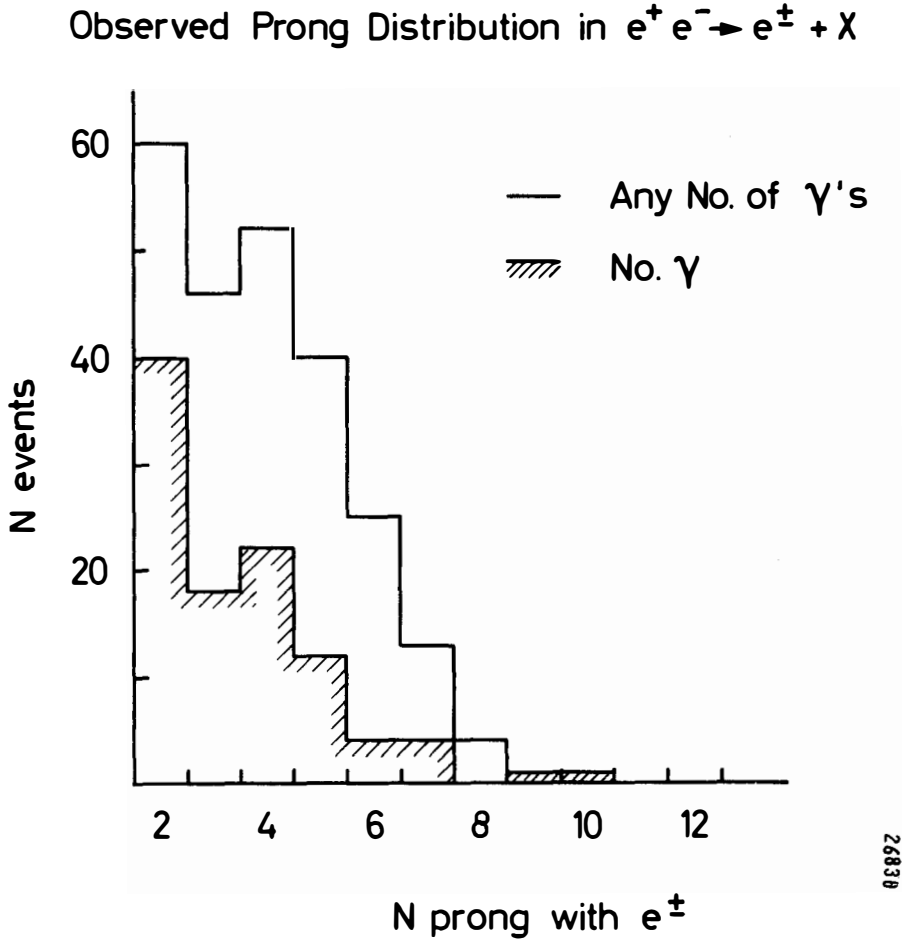

5.1 The charged track distribution observed by DASP[12,13] for inclusive electron events. The electron is included in the prong number. The shaded distribution is for events without photons.

5.2 Electron multiprong events and semileptonic decays of charmed particles

The properties of semileptonic decays of charmed particles were deduced from the electron multiprong events. The lepton spectrum associated with the multiprong sample is shown in Fig. 5.2. The estimated background due to hadron misidentification or heavy lepton production is also plotted. The background was scaled from measurements below threshold. The heavy lepton contribution was estimated assuming a τ branching ratio of 30 % to decay into final states with three or more charged particles. It was found that less than 12 % of the events with $n_{ch} \geq 3$ can be explained as heavy lepton production. The simple cut on hadron multiplicity therefore yields a rather clean sample of charm decays.

The electron spectrum contains information on the semileptonic and the leptonic decay modes of the lowest mass charmed hadrons. Fig. 5.2 demonstrates that semileptonic decays are much more important than leptonic decays because the latter, being two body decays, would produce a peak in the electron spectrum around 1 GeV/c. This is in gross disagreement with the data which peak around an electron momentum of 0.5 GeV/c with only few events above 0.7 GeV/c. To study the observed momentum spectrum in more detail we consider the spectrum obtained for cm energies between 3.99 GeV and 4.08 GeV. The charm cross section in this energy region is dominated by $D\bar{D}^*$ and $D^*\bar{D}^*$ production and is below the threshold for F production. The spectrum, corrected for the background and the heavy lepton contribution, is shown in Fig. 5.3.

The spectrum in Fig. 5.3 was fitted to three possible channels: $D \to e\bar{\nu}_e\pi$, $D \to e\bar{\nu}_e K$ and $D \to e\bar{\nu}_e K^*(892)$. A V-A current was assumed and the form of the spectra was taken from a paper by Ali and Yang[16]. Note that the theoretical spectra are model dependent. These fits gave a χ^2 value for 10 degrees of freedom of: 29.6 for $D \to e\bar{\nu}_e\pi$, 6.3 for $D \to e\bar{\nu}_e K$ and 2.8 for $D \to e\bar{\nu}_e K^*(892)$. The decay $D \to e\bar{\nu}_e\pi$ can therefore be excluded as the sole semileptonic decay mode of the D. The data can be fitted with either $D \to e\bar{\nu}_e K$ or $D \to e\bar{\nu}_e K^*(892)$.

The absolute cross section for inclusive electron production $e^+e^- \to e^\pm + X$, where X contains at least two charged tracks and any number of photons, is plotted in Fig. 5.4a as a function of energy. The data have been corrected for radiative effects. The background from hadron misidentification and the contribution from heavy leptonic production have been subtracted.

The inclusive cross section due to charmed particle production can be written as:

$$\sigma(e^+e^- \to e^\pm X) = \Sigma_{i,j}\, \sigma(e^+e^- \to C_i\bar{C}_j) \cdot \{B(C_i \to e\bar{\nu}_e X) + B(\bar{C}_j \to e\bar{\nu}_e X)\}$$

Here $(e^+e^- \to C_i\bar{C}_j)$ denotes the effective cross section for producing the

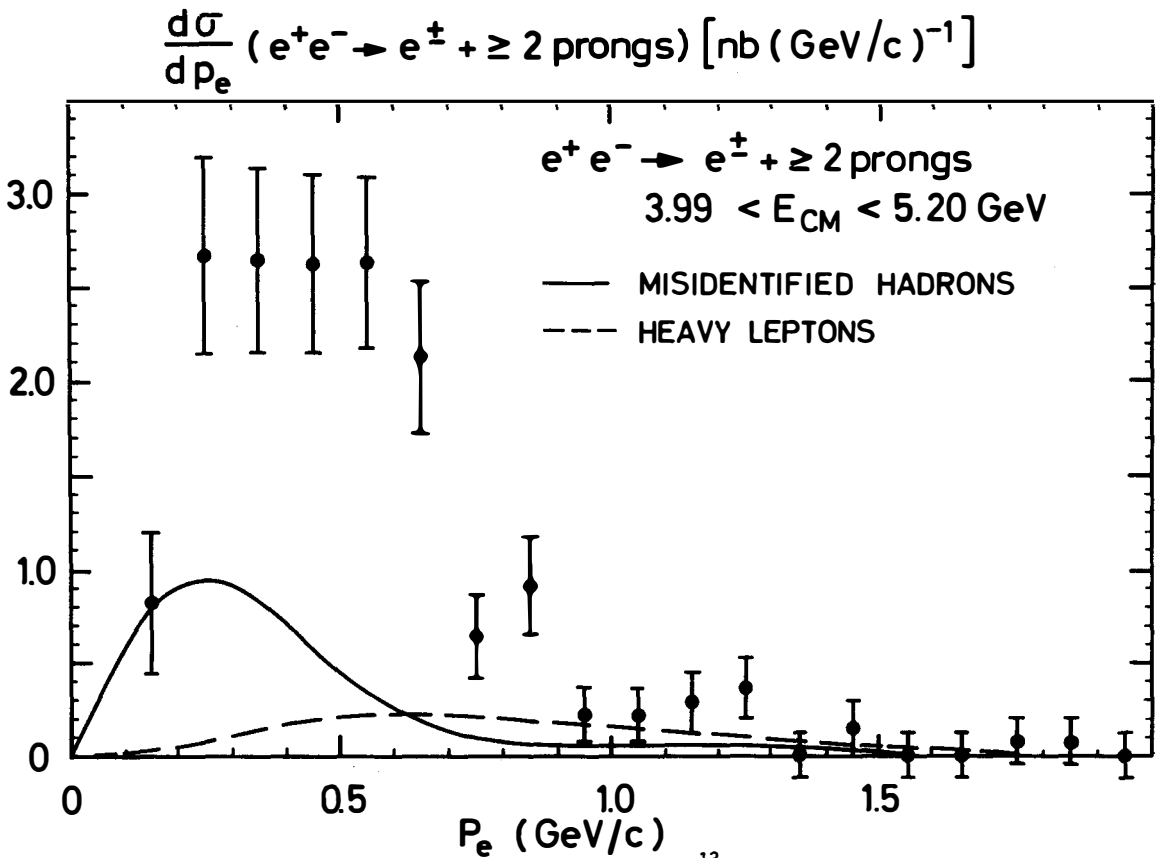

5.2 The inclusive electron momentum spectrum measured by DASP[13] between 3.99 GeV and 5.2 GeV for multi-prong events.

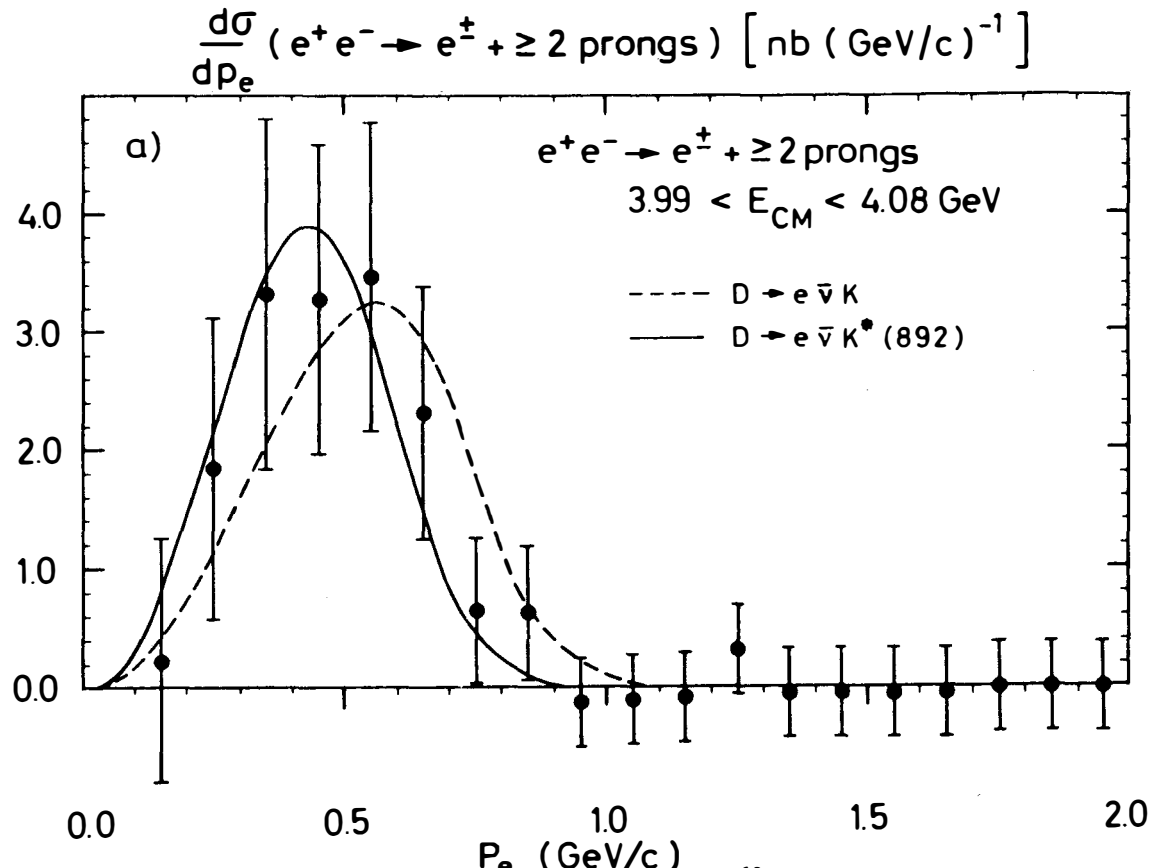

5.3 The electron momentum spectrum for $D \to e\nu X$ as measured by DASP[13]. The momentum distribution expected for $D \to e\bar{\nu}_e K$ and $D \to e\bar{\nu}_e K^*(892)$ are shown by the dashed and the solid curves.

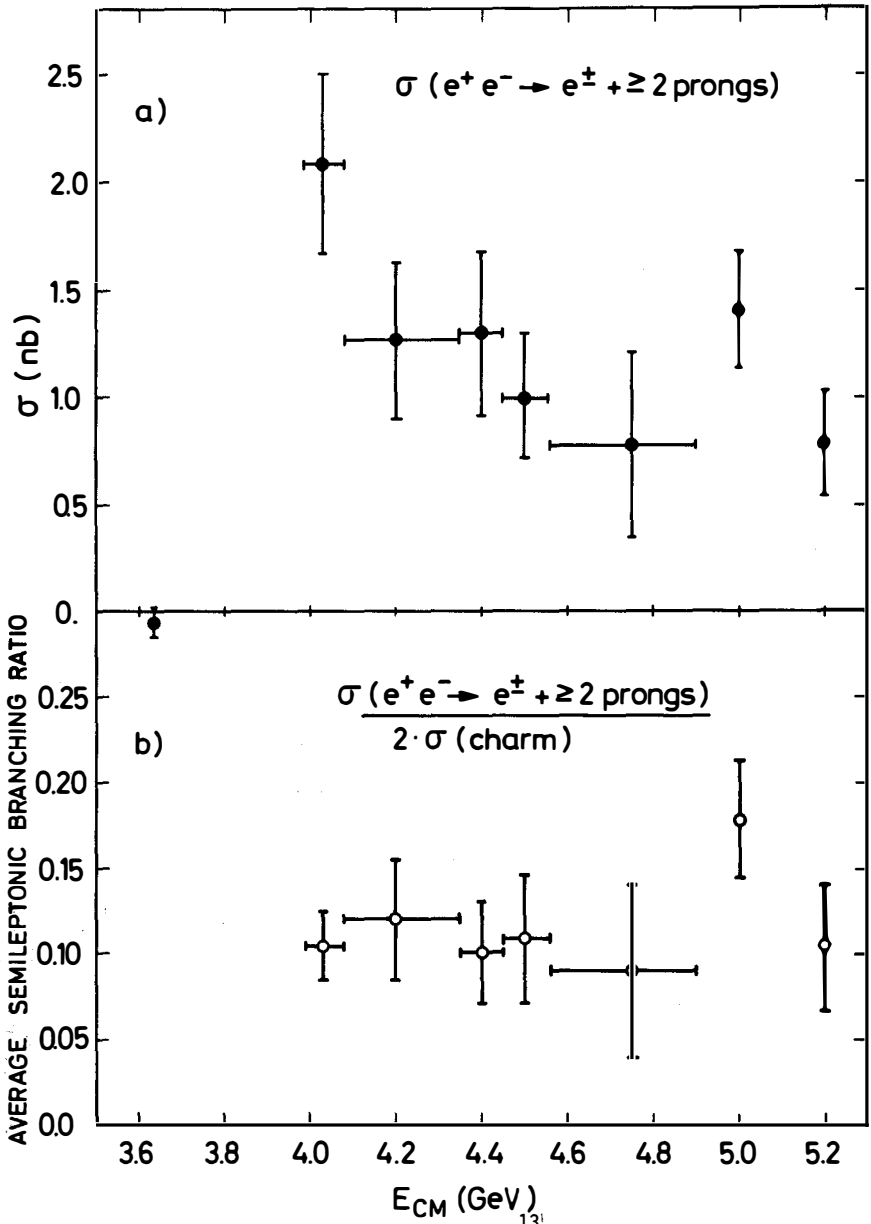

5.4 a) The cross section measured by DASP[13] for the inclusive production of electrons plus nonshowering track plus additional charged tracks as a function of cm energy.
b) The average semileptonic branching ratio for charmed hadrons as a function of energy. The error bars are statistical only.

lightest charmed hadron stable against strong and electromagnetic decays. These particles might either be produced directly or result from the cascade decay of excited charmed hadrons. The cross section $\sigma(e^+e^- \to C_i\bar{C}_j)$ was obtained by subtracting the cross sections for "old" hadron production from the total hadronic cross section.

Near threshold, where only neutral and charged D production can contribute DASP finds:

$$B(D \to e + X) = 0.08 \pm 0.02$$

This should be compared to the value

$$B(C \to e + X) = 0.072 \pm 0.02$$

obtained by avering over all energies between 3.9 GeV and 5.2 GeV (see Fig.5.4b). These values were extracted using the DASP[1] data for the total cross section and the error quoted is mainly systematic. Evaluating the branching ratio using the SPEAR data[17] on the total cross section as input led to an average semileptonic branching ratio of 0.08 ± 0.03, compared to 0.11 ± 0.03 obtained using the PLUTO[18] total cross section.

The semileptonic branching ratio can also be determined from the fraction of inclusive electron events containing a second electron. Using this method the DASP group finds $B(C \to e^-X) = 0.16 \pm 0.06$. Note that this value is independent of the charm cross section.

The semileptonic branching ratio of D's as measured by DASP is in accord with the results by LBL-SLAC[19] and the preliminary analysis of DELCO[20] (see Table 5.3).

Table 5.3 Semileptonic branching ratio of D mesons

Experiment	$B(D \to eX)$
DASP[13]	8 ± 2 %
DELCO[20]	11 ± 3 %
LBL-SLAC[19]	7.2 ± 2.8 %

The semileptonic branching ratio is larger than the value of 4 % predicted[21] from the weak decays of strange particles. This indicates that the mechanism responsible for enhancing the nonleptonic channels in strange particle decays are less effective[22] for charmed particle decays. In fact if none of the available channels are selectively enhanced one expects a semileptonic branching ratio of 0.20. This number is obtained by simple counting: the W decay can proceed in five different ways, $W \to e\nu$, $\mu\nu$ and $q\bar{q}'$ times three because of three

different colours: Assuming the same coupling strength, each channel has the probability 1 : 5 = 20 %.

One event was found by DASP with 3 electrons plus hadrons[13]. This number is consistent with the expected background leading to an upper limit of

$$(e^+e^- \to 3e + X) < 0.1 \text{ nb},$$

with 90 % confidence. Events of that type could arise from a charm changing neutral current, which allows a charmed hadron to decay into two electrons plus hadrons[23]. A neutral lepton paired with the electron in a right handed doublet would also yield events with three electrons and hadrons[22].

DASP[12] has determined the number of charged kaons emitted in electron multihadron events. This provides an independent consistency check on the nature of the weak current responsible for charm decay. If it is the GIM current then almost every electron event will have a $K\bar{K}$ pair. The measurement was done with events that had an identified charged hadron (π, K or $\bar{p}$) in the magnetic spectrometer, an electron in the inner detector and possibly other charged particles or photons. No $e\bar{p}X$ events were seen. From the observed K to π ratio and the measured charged multiplicity it was found that each multiprong event contained on the average 0.90 ± 0.18 charged kaons per event in agreement with the GIM prediction.

6. τ production

Measurements on lepton events of the type

$$e^+e^- \to e\mu + \text{nothing} \qquad (6.1)$$

and $e^+e^- \to e(\mu)$ + nonshowering charged particle + any number of photons (6.2)

provided convincing evidence that besides charmed particles a new type of weakly decaying particle, τ, is being produced above 4 GeV [24]. Conclusive proof for its existence was recently given by the DASP collaboration who observed τ production below charm threshold at the ψ'.

6.1 τ production below charm threshold

τ production at the ψ' was studied with electron twoprong events (6.2). The selection criteria for this sample were discussed in the previous section. A total of 17 events were found at the ψ' and 1 event at a cm energy of 3.6 GeV.

The electron momentum spectrum measured at the ψ' and plotted in Fig. 6.1 shows two clear clusters of events, one centered around 1.5 GeV/c and

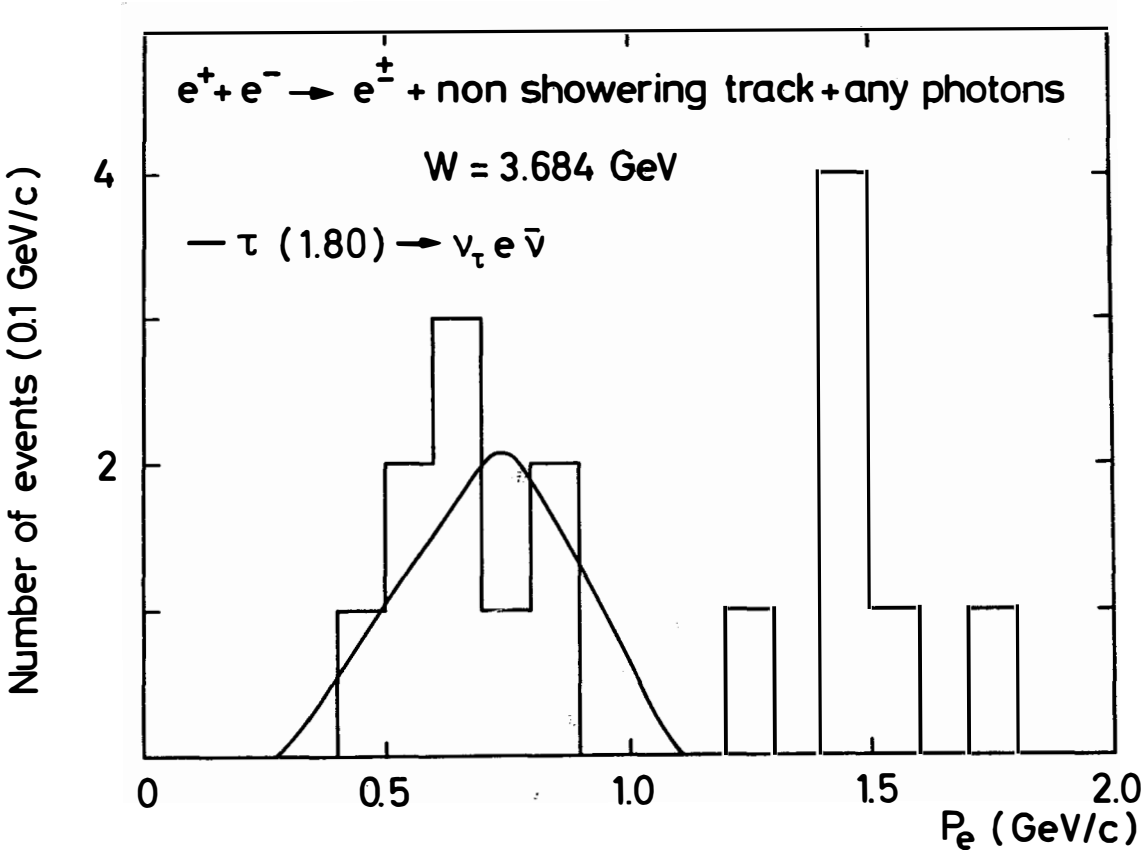

6.1 Raw electron momentum distributions observed by DASP[14] at 3.684 GeV. The events here are identified as electron, one nonshowering particle and any number of photons.

the other with momenta between 0.4 GeV/c and 0.9 GeV/c. The first cluster can be associated with the cascade decay $\psi' \to J/\psi\ X \to e^+e^-X$.

The electrons in the second cluster have a relatively flat momentum distribution. The background from the reaction $e^+e^- \to e^+e^-\mu^+\mu^-$ has been estimated to contribute (0.6 ± 0.2) events. An estimate using data at other energies shows that we expect less than 0.1 event from beam-gas interactions. Indeed, all the events originate within the nominal interaction volume. A twobody hadron final state can fake events of type (1) if the charged hadron traversing the magnet is misidentified as an electron. For hadrons with momenta above 0.35 GeV/c the measured probability P_{he} for this to happen is 4×10^{-4}. At the ψ' resonance 2113 events were observed of the type $e^+e^- \to h^\pm$ + nonshowering track + $\geq$ 0 photons where h is either a kaon or a pion traversing the magnet and the nonshowering track is observed in the inner or outer detector. This class of events therefore contributes a background of (0.84 ± 0.02) events. Dalitz decays of π^0 and η and photons converting in the beam pipe were estimated using the two prong sample above. A total of (0.2 ± 0.1) events were estimated compared to 9 events observed. The computation of background associated with multihadron events was checked by searching for inclusive electron events at the J/ψ resonance. One event of the type $e^+e^- \to e^\pm$ + nonshowering track + $\geq$ 0 photon was found which is to be compared with an estimated background of 1.3 events.

Further evidence that the electron events observed at the ψ' are not true hadron events comes from an inspection of the photon multiplicity. Table 6.1 shows a comparison of the photon multiplicities for twoprong electrons (0.4 GeV/c < p_e < 0.9 GeV/c) and twoprong hadron events (p_h > 0.4 GeV/c) from ψ' decay.

Table 6.1 Photon multiplicity distributions

Number of photons	0	1	2	3	4	5	6	7
$e^\pm$ + nonshowering track at the ψ'(0.4 < p_e < 0.9 GeV/c)	4	3	1	1	0	0	0	0
$h^\pm$ + nonshowering track at the ψ'(p_h > 0.4 GeV/c)	207	370	440	428	312	199	99	32
$e^\pm$ + nonshowering track $\sqrt{s}$: 4-5.2 GeV (p_e > 0.2 GeV/c)	49	17	10	1	2	0	1	0

The distributions are strikingly different. The electron events are accompanied by a few events as expected for τ decay whereas the hadron events have a large multiplicity.

We conclude therefore that an anomalous electron signal is observed at a cm energy of 3.684 GeV which is below charm threshold. This signal is then assumed to come from $\tau\bar{\tau}$ production. The electron spectrum predicted for a τ of mass 1.80 GeV and a zero mass neutrino fits the data well (see curve in Fig. 6.1).

6.2 τ production above 4 GeV

We turn now to the electron twoprong data at higher energies. A total of 80 events were found at cm energies between 4.0 and 5.2 GeV. A fraction of the twoprong electron events observed above 3.9 GeV might result from associated production and semileptonic decays of charmed particles. An upper limit can be obtained by assuming that all inclusive electron events with more than two prongs are due to charm production. From the measured multiplicity distribution of these events (Fig. 5.1) and the known detection efficiency a total of (5 ± 2) events has been estimated from this source. The direct decay of a pair of charmed hadrons into a final state with one electron and one non-showering track is expected to contribute less than one event. The background from all other sources has been estimated to (9 ± 3) events, in agreement with (7 ± 7) events extrapolated from the 3.6 GeV data.

6.2.1 τ mass and spin

The quantity $2\sigma_{\tau\bar{\tau}}\, B_e \cdot B_{ns}$ is plotted in Fig. 6.2 as a function of cm energy. Radiative corrections were applied and the data were corrected for the enhancement at the ψ' due to vacuum polarization. Note the rapid rise near threshold which is characteristic for s-wave production. The data shown in Fig. 6.2 were used to determine the mass of the τ and its spin[14]. The cross section for $\tau\bar{\tau}$ production for a τ spin of 0, 1/2 and 1 reads as follows:

spin 0:

$$\sigma_{\tau\bar{\tau}} = 1/4\ \sigma_{\mu\mu}\ \beta_\tau^3\ |F|^2\ B_e \cdot B_{ns} \qquad (6.3)$$

where $\sigma_{\mu\mu} = \frac{4\pi\alpha}{3s}$ and F is the τ formfactor.

spin 1/2:

$$\sigma_{\tau\bar{\tau}} = \sigma_{\mu\mu}\ \beta_\tau \left\{1 + 1/2\ (1-\beta_\tau^2)\right\}\ B_e \cdot B_{ns} \qquad (6.4)$$

The τ is assumed to be pointlike.

Spin 1 :

$$\sigma_{\tau\bar{\tau}} = \sigma_{\mu\mu}\ \beta_\tau \left\{\left(\frac{s}{4M_\tau^2}\right)^2 + 5\ \frac{s}{4M_\tau^2} + 3/4\right\} \cdot B_e \cdot B_{ns} \qquad (6.5)$$

The τ is assumed to have the same electromagnetic properties as the W boson[25].

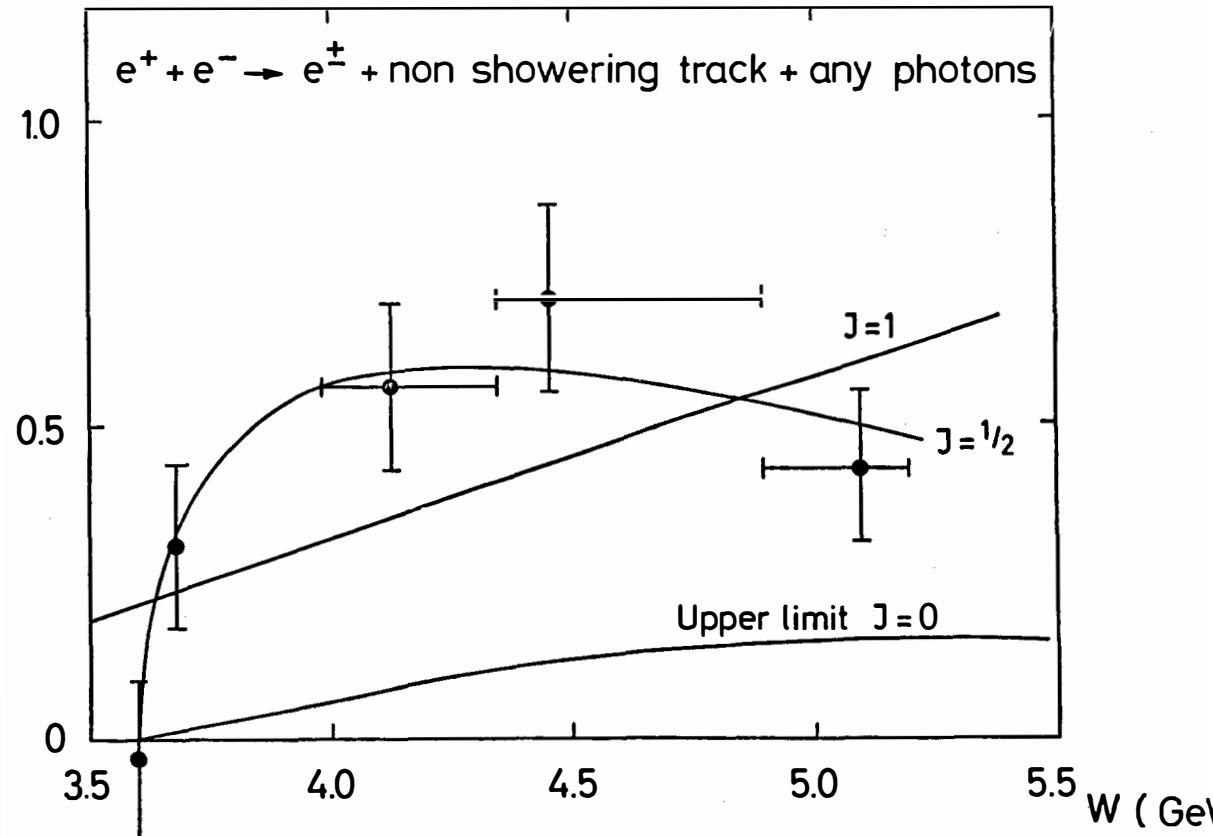

6.2 Integrated inclusive cross section for events having an identified electron, a nonshowering particle, and any number of photons as a function of cm energy. The data are from DASP[14]. The solid curves show fits to the data assuming pairproduction of point particles with spin 0, 1/2 and 1.

For spin 0 the upper limit on $2\sigma_{\tau\tau} B_e B_{ns}$ was calculated with F = 1 and the conservative assumption that the τ has only leptonic decays and $B_e = B_\mu$. This upper limit is plotted in Fig. 6.2 und is seen to be lower than the data by an order of magnitude. For spin 1/2 and 1 a fit was made treating the τ mass and the products of the branching ratios $B_e \cdot B_{ns}$ as free parameters. The spin 1 curve (see Fig. 6.2) does not describe the data; including the data obtained at higher energies at SPEAR excludes spin 1. The data are well described by a pointlike fermion of spin 1/2. The fit yielded for the τ mass

$$m_\tau = 1.807 \pm 0.02 \text{ GeV}.$$

6.2.2 The lepton momentum spectrum

Besides electron inclusive events the DASP group studied also μ inclusive events[14]. Candidates for muon inclusive events had to have one muon track in the spectrometer, a second nonshowering track and any number of photons observed either in the inner detector or in the spectrometer arms. A charged particle was called a muon if it had a momentum greater than 1.0 GeV/c, gave no signal in the threshold Cerenkov counter, suffered an energy loss consistent with that of a minimum ionizing particle in the shower counter and penetrated at least 60 cm of iron. A total of 25 events with a background of 3.8 events was found.

After all corrections (21 ± 5) muon inclusive events and (18.5 ± 4.6) electron inclusive events were observed with momenta above 1.0 GeV/c. The ratio of the leptonic widths evaluated directly from these data are independent of the form of the coupling. This yields $B_\mu/B_e = 0.92 \pm 0.32$ with a systematic uncertainty of 0.07. The result is consistent with $e\mu$ universality.

The lepton momentum spectrum, obtained by combining the electron and the muon data, is plotted in Fig. 6.3 for cm energies between 4.0 GeV and 5.2 GeV. This spectrum extends to much higher momenta than the electron spectrum observed in the semileptonic decays of the charmed hadrons, reflecting the pointlike structure of the τ and the low mass of its neutrino.

The solid line shows a fit to the data assuming $m_\tau = 1.80$ GeV, a massless neutrino and a (V-A) structure of the current. The dotted line is a fit keeping the masses constant but changing the left handed V-A current into a right handed V+A current. Both fits are clearly acceptable.

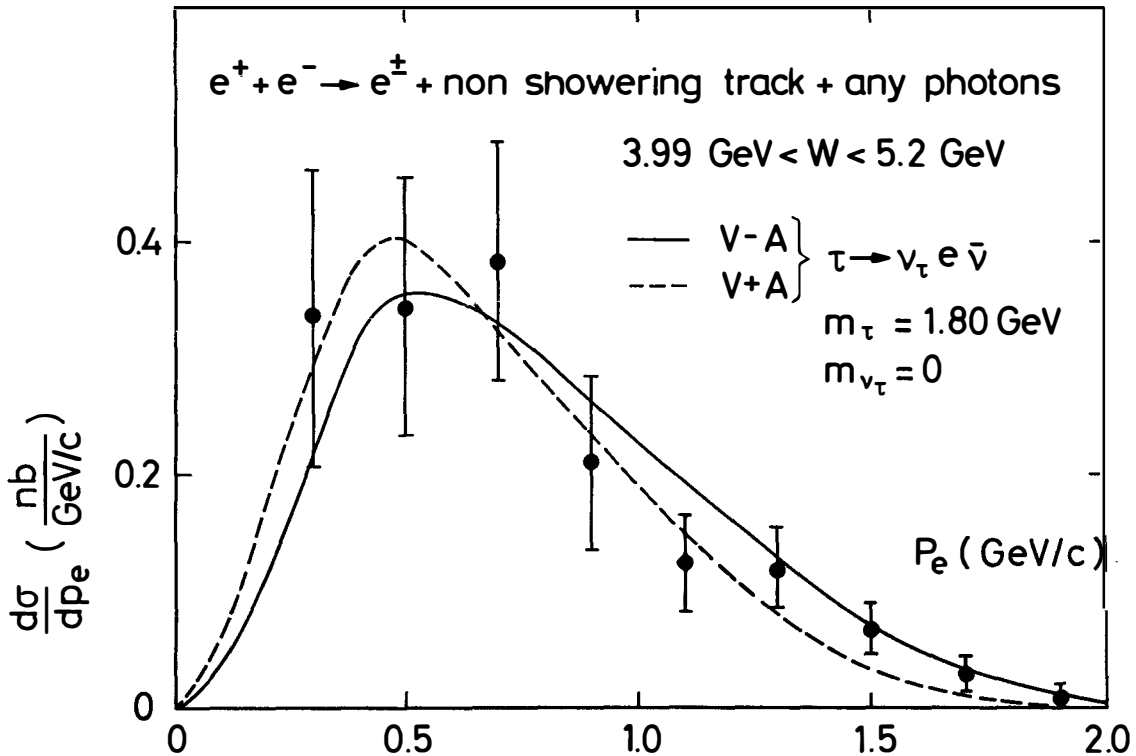

6.3 Corrected electron momentum distribution measured by DASP[14] for events having an identified electron, a nonshowering particle, and any number of photons. (Above 1 GeV/c data having a muon instead of an electron are combined with the electron data to form a weighted mean.)

6.3 Leptonic and topological τ decay branching ratios

The DASP group measured[14] $e^+e^- \to e\mu$ + missing energy in the cm range of 0.4 GeV to 5.2 GeV. Muons of momenta greater than 0.7 GeV/c were identified in the outer detector ($P_{h\mu} = 4.2 \pm 0.8$ %) by range, electrons with momenta above 0.2 GeV/c either in the inner detector ($P_{he} = 2 \pm 0.9$ %) or the outer ($P_{he} = 4 \times 10^{-4}$). A total of 13 $e\mu$ events with an estimated background of 1.2 ± 0.4 events were found. Using the known production cross section and assuming $e\mu$ universality yield:

$B_e = B_\mu = 0.182 \pm 0.028 \pm 0.014$ for a V-A current and

$B_e = B_\mu = 0.206 \pm 0.033 \pm 0.015$ for a V+A current. The first error is the statistical one.

The fit used to evaluate the τ mass from the electron inclusive events yields $B_e \cdot B_{ns} = 0.086 \pm 0.012$. Using $B_e = 0.182 \pm 0.028$ the DASP group derived the branching ratio for $\tau \to \nu_\tau$ + nonshowering particle + ≥ 0 photons, $B_{ns} = 0.47 \pm 0.10$. The branching ratio B_{1h} for $\tau \to \nu_\tau$ + hadron + ≥ 0 photons is given by $B_{1h} = B_{ns} - B = (0.29 \pm 0.11)$. The systematic errors are small compared to the statistical error. The average number of photons associated with $\tau \to \nu_\tau$ + hadron + ≥ 0 photons can be obtained from table 6.1 after making background corrections. Averaging the observed photon multiplicity over all two prong events in the higher energy data and correcting for the photon detection efficiency the decay of the type $\tau \to \nu_\tau$ + charged hadron + any number of photons was found to yield on the average 2.8 ± 0.7 photons.

The branching ratio B_{3h} for the τ to decay into final states with at least three charged particles can be obtained from $B_{3h} = 1 - B_e - B_{ns}$. (The number of electron events with $p_e > 1$ GeV/c and 5 or more charged tracks were found to be small.) The result is $B_{3h} = 0.35 \pm 0.11$ in agreement with the Pluto[26] measurement, B(≥ 3 prong) = 0.30 ± 0.10.

Fits were also made varying the mass of the τ neutrino. The 90 % confidence upper limits on the neutrino mass are $m_{\nu_\tau} < 0.74$ GeV for V-A and $m_{\nu_\tau} < 0.54$ GeV for V+A.

6.4 Semihadronic decays of the τ

A characteristic feature of the standard weak interaction is that decays involving strange particles are suppressed relativ to decays involving nonstrange final states by $tg^2\theta_c \approx 0.05$. The DASP group determined[12] the ratio of strange to nonstrange particles in semihadronic τ-decays from a measurement of

$$\frac{\sigma(e^+e^- \to e^{\mp} + K^{\pm} + \geq 0 \text{ photons})}{\sigma(e^+e^- \pm e^{\mp} + \pi^{\pm} + \geq 0 \text{ photons})}$$

It was shown that the two prong cross section including one electron predominately results from $e^+e^- \to \tau\bar{\tau} \to (\nu_\tau e\bar{\nu}_e)(\nu_\tau + \text{hadrons} + \geq 0 \text{ photons})$ with only a small contamination from charm decays. The hadrons were identified and measured using one of the spectrometer arms. The electron was identified in either the inner or the outer detector.

The results was

$$\frac{\sigma(e^{\mp} + K^{\pm} + \geq 0 \text{ photons})}{\sigma(e^{\mp} + \pi^{\pm} + \geq 0 \text{ photons})} = 0.07 \pm 0.06$$

Therefore on the average only 7 % of all semihadronic τ-decays yield a strange particle in accordance with theory. This should be compared to multiprong events where DASP found[12]:

$$\frac{\sigma(e^{\mp} + K^{\pm} + \geq 1 \text{ prong} + \geq 0 \text{ photons})}{\sigma(e^{\mp} + \pi^{\pm} + \geq 1 \text{ prong} + \geq 0 \text{ photons})} = 0.24 \pm 0.05.$$

Since the charged multiplicity is on the order of 4 this is equivalent to (0.9 ± 0.18) charged kaons per multiprong event. (See discussion in section 5.)

6.4.1 $\tau \to \pi\nu$

We have searched[27] for the $\tau \to \pi\nu$ decay by studying the process

$$e^+e^- \to \tau\bar{\tau} \to (e\nu\nu)(\pi\nu)$$

leading to the final state $e\pi^{\pm}\,0\gamma$. In order to reduce background from charm production only cm energies W > 4.48 GeV were considered. The electron was detected in the inner detector or in the magnetic spectrometer, the $\pi^{\pm}$ was identified in the magnetic spectrometer. To enhance the $\tau \to \pi\nu$ signal only $\pi^{\pm}$ with momenta above 1.1 GeV/c were considered. Two events satisfying these selection criteria were observed.

From $\tau\bar{\tau}$ production 6.7 events were expected plus 1 event from background (e.g. $\tau \to \rho\nu$ where the π^0 from τ decay escaped detection). The difference between expected and observed number of events corresponds to a 2 s.d. effect. The observed number of events lead to

$$B_e \cdot B_\pi = 0.004 \,{}^{+\,0.005}_{-\,0.004}$$

or

$$B_\pi = 0.02 \,{}^{+\,0.03}_{-\,0.02}$$

which can be compared to the theoretical value of $B_\pi = 0.10$. The data from SLAC-LBL presented at this meeting[28] suggest, however, that the $\pi\nu$ decay exists with the expected strength.

The DASP group has also searched for events of the type

$$e^+e^- \to \tau\bar{\tau} \to \{(K\nu)\ (e\nu\nu) + (\mu\nu\nu) + (\pi\nu)\}$$

$$= K^\pm + \text{charged track} + \text{missing energy}.$$

Only one event with $p_K > 1.0$ GeV/c was found[27]. This yields a 90 % confidence upper limit of $B_K < 0.016$.

6.4.2 $\tau \to \rho\nu$

DASP measured[27] the decay $\tau \to \rho\nu_\tau$ by selecting final states with $\pi^\pm$ + charged track + two photons. Events in which the two photons are compatible with resulting from a π^0 decay are retained provided that both computed photon energies are above 50 MeV. The remaining events are plotted versus $M(\pi^\pm\pi^0)$ in Fig. 6.4a. Events with an identified electron are hatched. Events within the ρ-band (0.5 GeV < $M(\pi^\pm\pi^0)$ < 1.0 GeV) are plotted versus the momenta of the $\pi^\pm\pi^0$-system in Fig. 6.5. The momentum distribution expected from the decay $\tau \to \rho\nu_\tau$ is shown as the dotted line. Note the flat distribution above 0.9 GeV/c which is characteristic for a two body decay of a moving object. The enhancement at low momenta is presumably due to multihadron events. To reduce the background, only events with a $(\pi^\pm\pi^0)$-momentum above 1.0 GeV/c are considered. The $\pi^\pm\pi^0$ mass distribution for these events are plotted in Fig. 6.4b. These events yield as a preliminary value

$$B_\rho = 0.24 \pm 0.09$$

in good agreement with the theoretical prediction, $B_\rho = 0.22$.[29]

6.5 Summary of the τ properties

Table 6.2 summarizes the information on mass, leptonic and semi-hadronic decay modes of the τ from this and other experiments.

The observation of the τ at the ψ' below charm threshold conclusively demonstrates that the τ signal has nothing to do with charm. The shape and magnitude of the $\tau\bar{\tau}$ production cross section exclude spin 0 and 1 for the τ: they strongly favor the assignment as a pointlike, spin 1/2 fermion. The best value for the τ mass at present is 1.807 ± 0.02 GeV. The analysis of the decay spectra puts a limit of 0.54 GeV on the mass of the τ neutrino. The lifetime of the τ is less than $3.5 \cdot 10^{-12}$ sec.

The lepton momentum spectra can be described by a V-A as well as a V+A coupling of the weak current to the $\tau\bar{\nu}_\tau$ system although the first possibility is

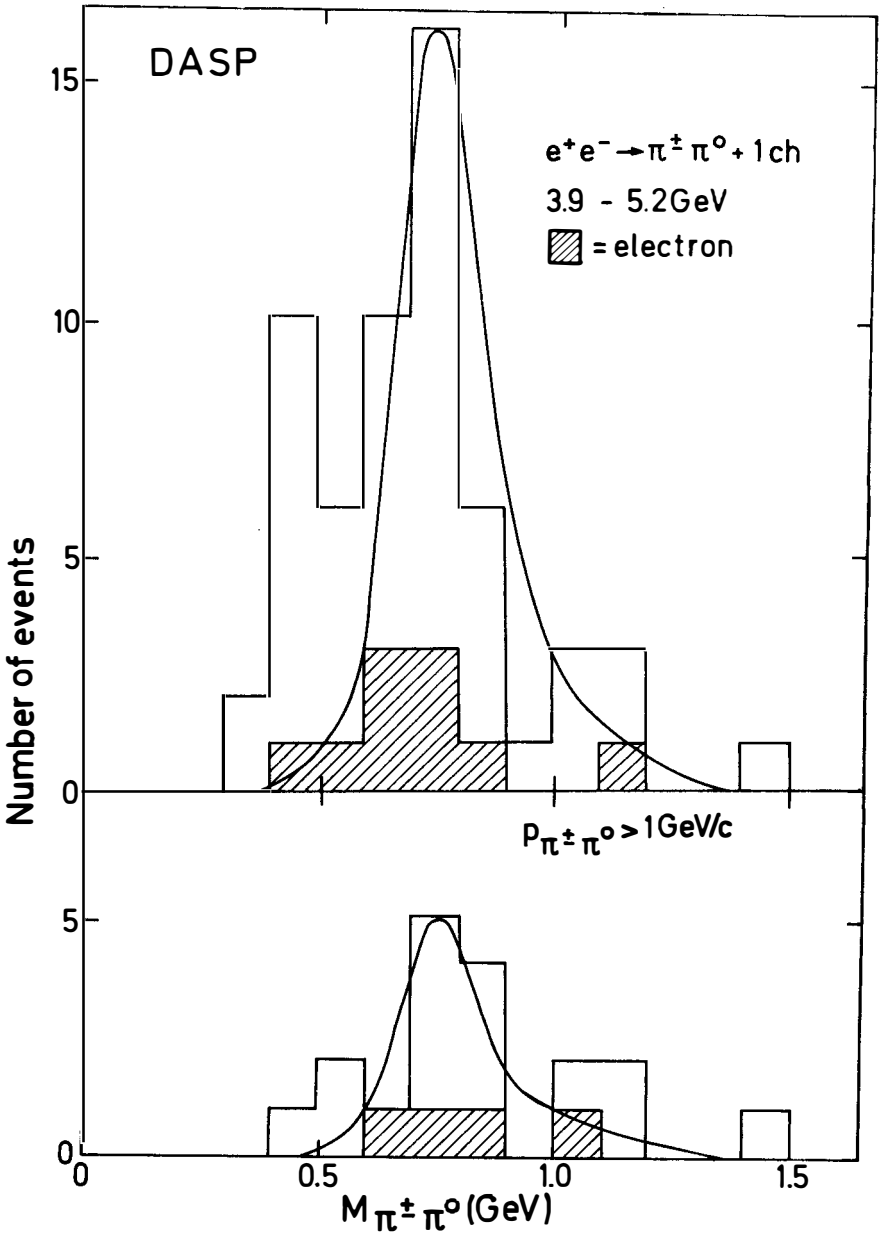

6.4 a) The distribution of $M(\pi^\pm\pi^o)$ observed by DASP[27] for events with the topology $e^+e^- \rightarrow \pi^\pm\pi^o$ + charged track.
b) The $M(\pi^\pm\pi^o)$ distribution for events of the same topology as above but with $p_{\pi^\pm\pi^o} > 1$ GeV/c.

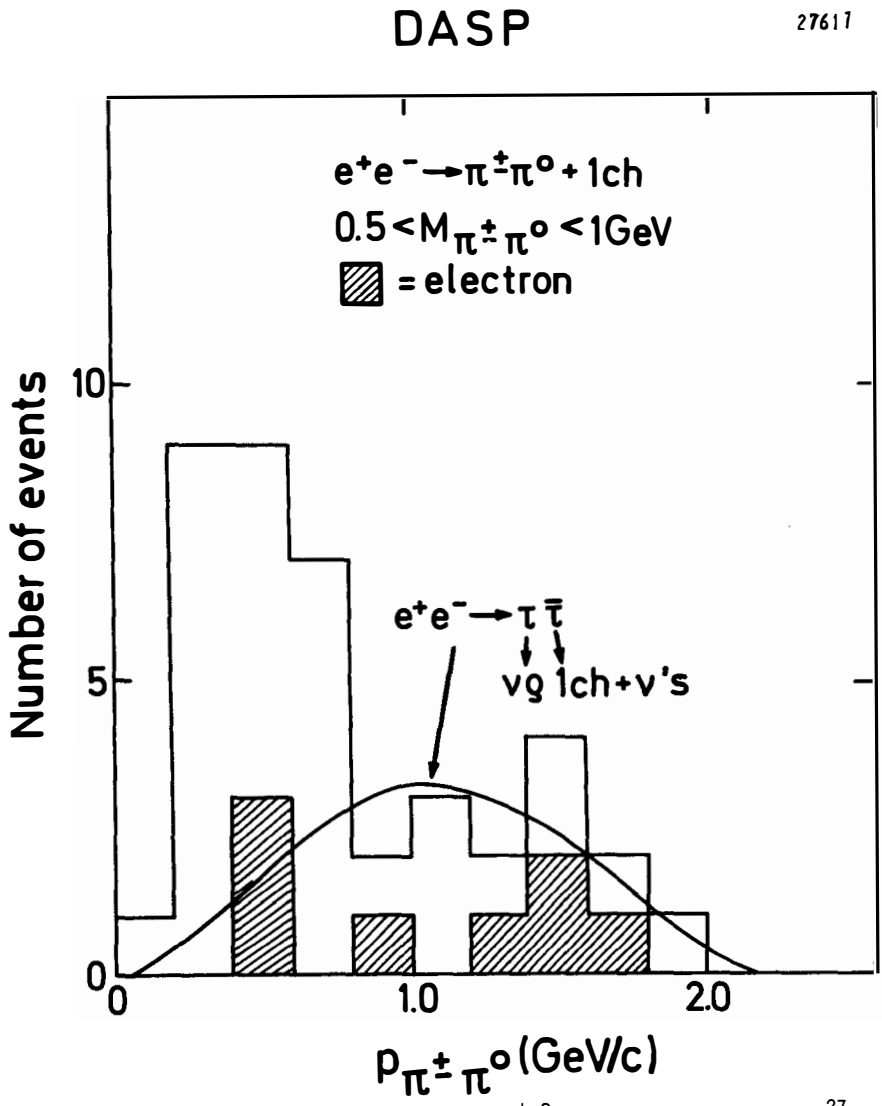

6.5 The momentum distribution of the $(\pi^{\pm}\pi^{0})$ system observed by DASP[27] in $e^{+}e^{-} \rightarrow \pi^{\pm}\pi^{0}T$. The mass of the $\pi^{\pm}\pi^{0}$ system was between 0.5 GeV and 1.0 GeV.

Table 6.5 Properties of the

	experimental results	predicted by theory	experiment	comments
mass (GeV)	1.807 ± 0.020		DASP[14]	
Spin	1/2			
lifetime (sec)	$<3.5\cdot10^{-12}$	$2.8\cdot10^{-13}$	PLUTO[30]	
m_{ν_τ} (GeV)	<0.54		SLAC-LBL[31], PLUTO[30]	
$\tau\nu_\tau$ coupling to weak current	V-A favored		SLAC-LBL[31], PLUTO[26]	
B_μ / B_e	0.92 ± 0.32	1 (seq.lept.)	DASP[14]	
B_e	0.186 ± 0.010 ± 0.028	0.18	SLAC-LBL[32]	from $e\mu$; assume B_e = B and V-A
	0.16 ± 0.06		PLUTO[30]	from $e\mu,\mu X$; assume V-A
	0.224 ± 0.032 ± 0.044		LBL-SLAC[33]	from $e\mu$; assume B_e = B
	0.182 ± 0.028 ± 0.014		DASP[14]	from $e\mu$; assume B_e - B and V-A
	0.15		DELCO[20]	from eX; preliminary
B_μ	0.175 ± 0.072 ± 0.030	0.18	SLAC-LBL	from μX; assume B_{18} = 0.85 and V-A
	0.14 ± 0.034		PLUTO[26]	from μX; assume V-A
	$0.22\ ^{+\ 0.07}_{-\ 0.08}$		Iron ball[35]	from $\mu\mu$
	0.20 ± 0.10		Maryland-Princeton -Pavia	from μX
$B(\tau \to e\gamma)$	<0.026		LBL-SLAC[31]	
$B(\tau \to \mu\gamma)$	<0.013		LBL-SLAC[31]	
B(τ → 3 charged leptons)	<0.006		SLAC-LBL[31]	
	<0.01		PLUTO[36]	

Table 6.5 continued

	experimental results	predicted by theory	experiment	comments
$B(\tau \to 1$ charged + any photons)	0.70 ± 0.10		PLUTO[26]	
	0.90 ± 0.10		LBL-SLAC[33]	
	0.65 ± 0.12		DASP[14]	
$B(\tau \to 1$ charged hadron + any photons)	0.40 ± 0.15		PLUTO[26]	
	0.45 ± 0.19		LBL-SLAC[33]	
	0.29 ± 0.11		DASP[14]	
$B(\tau \to 3$ charged hadrons + any photons)	0.35 ± 0.11		DASP[14]	
$B(\tau \to \pi\nu)$	0.02 ± 0.03	0.10	DASP[27]	
$B(\tau \to k\nu)$	<0.016	0.005	DASP[12]	
$B(\tau \to \rho\nu)$	0.24 ± 0.09	0.22	DASP[27]	
$B(\tau \to \rho^0\pi^\pm\nu)$	0.050 ± 0.015	~0.1	PLUTO[30]	$\rho\pi$ sepctrum consistent with A_1 decay. Including neutral decay modes would give $B(\tau \to A_1\nu) = 0.10 \pm 0.03$

slightly favored by the data. The measured leptonic decay rates are consistent with e/μ universality. The leptonic and semihadronic branching ratios agree with those expected from theory for a heavy lepton of mass 1.8 GeV, except perhaps for the decay $\tau \to \pi\nu$ which needs further study.

The consistency with e/μ universality classifies the τ as either a ortholepton or a sequential lepton. In the first case the τ has the same lepton number as e or μ. In the second case the τ carries a new lepton number. Recent neutrino experiments rule out that the τ is μ-like[37] and strongly indicate that it is not e-like[38] either. The τ is therefore most probably a sequential heavy lepton with a new lepton quantum number and with its own neutrino.

ACKNOWLEDGEMENTS

I want to thank Profs. Tran Thanh Van and M. Davier for the invitation to give these lectures. In preparing them I have profitted from a close collaboration with Björn Wiik.

References:

The following shorthand notations shall be used: 1971 Cornell Conference for the Proceedings of the 1971 Symposium on Electron and Photon Interactions at High Energies, Cornell, ed. by N. Mistry.

1975 Stanford Conference for the Proceedings of the 1975 Symposium on Lepton and Photon Interactions at High Energies, Stanford, ed. by W.T. Kirk.

1976 Tbilisi Conference for the XVIIIth International Conference on High Energy Physics, Tbilisi, USSR (1976).

1977 Hamburg Conference for the Proceedings of the 1+77 International Symposium on Lepton and Photon Interactions at High Energies, Hamburgs, ed. by F. Gutbrod.

1) G. Grindhammer, Lecture given at this meeting.

2) The DASP results were summarized bv S. Yamada, 1977 Hamburg Conference, p.69.

3) R.F. Schwitters, rapporteur talk, 1975 Stanford Conference, p.5;
G. Hanson, rapporteur talk, 1976 Tbilisi Conference, and SLAC-PUB-1814 (1976).

4) DASP Collaboration, R. Brandelik et al., Phys. Lett. 67B (1977) 358 and paper to be published.

5) See e.g. S.D. Drell, D. Levy and T.M. Yan, Phys. Rev. 187 (1969) 2159;
ibid D1 (1970) 1035, 1616, 2402;
see also B.H. Wiik and G. Wolf, Electron-Positron Interactions in Les Houches, Session XXIX, 1976,
Interaction électromagnétiques et faibles à haute énergie/ Weak and electromagnetic interactions at high energy, ed. by R. Balian and C.H. Llewellyn Smith, Course 5, p. 407,

6) DASP Collaboration, W. Braunschweig et al., Phys. Lett. 63B (1976) 115.

7) R. Gatto, P. Menotti and I. Vendramin, Lettre Nuovo Cimento 5 (1972) 754;
R. Gatto and G. Preparata, Nucl. Phys. B47 (1972) 313.

8) V.N. Gribov and L.N. Lipatov, Yadernaya Fisika 15 (1972) 1218.

9) G. Hanson et al., Phys. Rev. Lett. 35 (1975) 609.

10) D. Fakirov and B. Stech, Heidelberg preprint HD-THEP-77-8 (1977) and Nucl. Phys.
H. Fritzsch, Phys. Lett. 71B (1977) 429.

11) DASP Collaboration, R. Brandelik et al., Phys. Lett. 70B (1977) 132 and
G. Mikenberg, Proceedings of the Triangle Seminar, 1977.

12) DASP Collaboration, R. Brandelik et al., Phys. Lett. 70B (1977) 125.

13) DASP Collaboration, R. Brandelik et al., Phys. Lett. 70B (1977) 387.

14) DASP Collaboration, R. Brandelik et al., Phys. Lett. 73B (1978) 109.

15) see e.g. B.H. Wiik, rapporteur talk, 1976 Tbilisi Conference.

16) a) I. Hinchliffe and C.H. Llewellyn Smith, Nucl. Phys. B114 (1976) 45
b) A. Ali and T.C. Yang, Phys. Lett. 65B (1976) 275
c) F. Bletzacker, H.T. Nieh and A. Soni, Phys. Rev. D16 (1977) 732
d) R. Nabari, X.Y. Pham and W. Cottingham, J. Phys. G: Nuclear Physics 3 (1971) 1485
e) G.L. Kane, Phys. Lett. 70B (1977) 272
f) X.Y. Pham and J.M. Richard, Preprint PARIS/LPTHE 77.20.

17) A.M. Boyarski et al., Phys. Rev. Lett. 34 (1975) 764;
R.F. Schwitters, 1975 Stanford Conference, p.5.

18) J. Burmester et al., Phys. Lett. 66B (1977) 395; and
G. Knies, rapporteur talk, 1977 Hamburg Conference, p. 93.

19) J.M. Feller et al., Phys. Rev. Lett. 40 (1978) 274 and
A. Barbaro-Galtieri, rapporteur talk, 1977 Hamburg Conference, p. 21.

20) DELCO Collaboration, J. Kirkby, rapporteur talk, 1977 Hamburg Conference, p.3.

21) M.K. Gaillard, B.W. Lee and J.L. Rosner, Rev. Mod. Phys. 47 (1975) 277.

22) J. Ellis, M.K. Gaillard and D.V. Nanopoulos, Nucl. Phys. B100 (1975) 313.

23) P. Fayet, Nucl. Phys. B78 (1974) 14;
T.D. Cheng and L.F. Li, Phys. Rev. Lett. 38 (1977) 381.

24) see e.g.M.L. Perl, review talk, 1977 Hamburg Conference, p. 145.

25) W. Alles, Ch. Boyer and A.J. Buras, CERN-TH 220 (1977).

26) PLUTO Collaboration, J. Burmester et al., Phys. Lett. 68B (1977) 297.

27) see S. Yamada, rapporteur talk, 1977 Hamburg Conference, p. 69.

28) G. Hanson and M.L. Perl, data of the SLAC-LBL Collaboration presented at this meeting.

29) H.B. Thacker and J.J. Sakurai, Phys. Lett. 36B (1971) 103;
Y.S. Tsai, Phys. Rev. D4 (1971) 2821;
J.D. Bjorken and C.H. Llewellyn Smith, Phys. Rev. D7 (1973) 887;
K. Fujikawa and N. Kawamoto, Phys. Rev. D14 (1976) 59;

Y.I. Azimov, L.L. Frankfurt and V.A. Khoze, Leningrad Nuclear Physics Institute, Preprint 245, June 1976;
N. Kawamoto and A.I. Sanda, DESY 78/14;
Similar results are reported also by:
F.J. Gilman and D.H. Miller, SLAC-PUB-2046, 1977 and
Y.S. Tsai, private communication.

30) PLUTO Collaboration, G. Alexander et al., Phys. Lett. 73B (1978) 99 and G. Knies, rapporteur talk, 1977 Hamburg Conference, p. 93.

31) M.L. Perl, rapporteur talk, 1977 Hamburg Conference, p. 145.

32) M.L. Perl et al., Phys. Lett. 70B (1977) 487;
M.L. Perl et al., Phys. Lett. 63B (1976) 466.

33) A. Barbaro-Galtieri, Phys. Rev. Lett. 39 (1977) 1058).

34) G.J. Feldman et al., Phys. Rev. Lett. 38 (1977) 117.

35) Contribution to the Hamburg Conference
see H. Sadrozinski, rapporteur talk, 1977 Hamburg Conference, p. 47.

36) See the recent review talks by
M.L. Perl, Proceedings of the XII Rencontre de Moriond, Flaine, 1977, to be published, and SLAC-PUB-1923;
and 1977 Hamburg Conference, p. 145;
G. Flügge, Invited talk at the Vth International Conference on Experimental Meson Spectroscopy, Northeastern University, Boston, MA, 1977, DESY-Report 77/35 (1975.

37) see e.g. K. Kleinknecht, rapporteur talk, 1977 Hanburg Conference, p. 271.

38) R. Palmer, results reported at this meeting.